



Washington University in St. Louis

JAMES MCKELVEY SCHOOL OF ENGINEERING

Spring 2024 MEMS 412 Design of Thermal Systems

Design Homework #3: Combined Cycle: CCGT

Course Instructor: Dr. Patricia Weisensee

I hereby certify that the lab report herein is our original academic work, completed in accordance with the McKelvey School of Engineering and Undergraduate Student academic integrity policies, and submitted to fulfill the requirements of this assignment:

Jacob Rapoza

A handwritten signature in black ink, appearing to read "Jacob Rapoza".

Problem Background

This design homework is analyzing a combined cycle gas turbine (CCGT) including a Brayton cycle as the topping cycle and a Rankine cycle as the bottoming cycle. The waste heat from the Rankine cycle is shared with the Brayton cycle through a series of heat exchangers.

1 Assumptions and Boundary Conditions

Below are some given and assumed boundary conditions carried over from Design Homework 1 (The Rankine cycle) and Design Homework 2 (The Brayton cycle and solar tower) as well as some new assumptions for Design Homework 3 (the CCGT).

1.1 Rankine Cycle Boundary Conditions/Assumptions.

- (1) Rankine cycle is a closed cycle with no mass flow into or out of the system.
- (2) The working fluid of the closed Rankine Cycle is water.
- (3) The coolant for the condenser is water from a river, lake, or ocean.
- (4) The power for the operation of the pump is part of the cost when optimizing the cycle efficiency.
- (5) Minor losses from the supplying pipe can be ignored.
- (6) Friction losses from flow through the condenser heat exchanger can not be ignored and must be included.
- (7) The condenser is a shell and tube condenser.
- (8) Steam turbines can operate safely at 10-12% moisture[1]. This is because steam turbine blades have high rotation speed. Higher moisture content would lead to increased droplet formation which will hit the blades and cause impact erosion over time.
- (9) The coolant water inlet temperature is 18.3 ° C. This is assumed because the water source chosen is the Missouri River at the Holter Dam in Montana. Specifically, it is assumed that the power generation will be occurring in July 2023 when the average water surface temp is about 65° F or 18.3° C [2].
- (10) The cooling water discharge temperature is 70° F or 21.1 ° C. This is assumed because the EPA says that water temperature discharge can at no point be more than 5° F above the surface water temperature [3].
- (11) The difference between the saturation temperature and the temperature of the cooling water is about 34° F. This is assumed because heat flows from hot to cold but you don't want a huge temperature difference split [4, 5]. It is specifically assumed to be 34° F so that the saturation temperature of the liquid at state 9 is a nice round 40° C.
- (12) The mass flow rate remains constant throughout the entire Rankine Cycle. This goes along with the system being a closed cycle but clarifies that no mass flow rate will be lost to minor losses, major losses, etc.
- (13) The condenser tubing is assumed to be a new copper tubing because these are the most common type due to their good processing performance and moderate cost [6]. Along with this the assumed surface roughness of the copper pipes is .0015 mm [7].

- (14) The state of the water entering the turbine is a super-heated vapor. This is assumed because the quality needs to be high thus we need dry vapor.
- (15) The state of the water entering the pump within the Rankine Cycle is saturated liquid. This is assumed because shell and tube condensers work on the basis of pooling saturated liquid at the bottom of their apparatus.
- (16) States 9→6 is an adiabatic compression (we will assume ideal so that entropy does not change), states 6 → 7 is an isobaric heating, states 8 → 9 is an isobaric cooling. We assume this because it simplifies everything but the turbine section of the Rankine cycle so that it is ideal.
- (17) The turbine has an isentropic efficiency of 90
- (18) The water pressure at the pump exit is 1000 kPa.
- (19) The high-temperature heat exchanger provides 30 MW of thermal energy.
- (20) The upper bound of the steam turbine inlet temperature is 400 °.
- (21) The heat transfer rate within the coolant in the condenser is $U = h_{coolant} = 1000 \frac{W}{m^2 K}$.
- (22) The quality of the steam at the turbine exit is 88%. This is chosen as the quality because it is the lower value for the range of the accepted quality for a utility-scale turbine [1]
- (23) The cooling water inlet temperature is 65° F or 18.3 ° C[2].
- (24) The cooling water discharge temperature is 70° F or 21.1° C [3].
- (25) The temperature split of the condenser is 34° F [6].
- (26) The water temperature at the outlet of the condenser (state 9) is 104° F or 40° C.
- (27) The lower bound of the steam turbine inlet temperature is 359.1° C because the turbine exit quality is 88% at this state assuming ideal isentropic conditions.

1.2 Brayton Cycle Boundary Conditions/Assumptions.

- (1) The Brayton cycle is an open cycle with mass flow into and out of the system.
- (2) The working fluid of the open Brayton cycle is air as an ideal gas.
- (3) The low-temperature heat exchanger gives off 30 MW of thermal energy.
- (4) The temperature of the air entering the compressor from the environment is $T_1 = 300K$.
- (5) The temperature of the air leaving the heater and entering the gas turbine is $T_3 = 1200K$.
- (6) The temperature of the air leaving the heat exchanger tied to the bottoming Rankine cycle is $T_5 = 500K$.
- (7) The realistic range of compression ratios is $r_p = \frac{p_2}{p_1} = 5 - 30$.
- (8) The isentropic efficiencies of the compressor and turbine vary from 70-100%.

1.3 Solar Tower Boundary Conditions/Assumptions.

- (1) The heliostats available for this system are 10m x 10m in size.
- (2) Assuming perfect solar-to-thermal conversion.
- (3) The power plant is located in Kailua Kona.
- (4) The monthly average direct normal solar irradiation in Kailua, Kona is $3.14 \frac{kWh}{m^2}$ per day which is $130.83 \frac{W}{m^2}$ [8].
- (5) A realistic compressor isentropic efficiency is 88% [9].

- (6) A realistic turbine isentropic efficiency is 93% [9].

1.4 Combined Cycle Gas Turbine Boundary Conditions/Assumptions.

- (1) Numbering of the different pressures and temperatures will refer to Fig. 3 .
- (2) The preheater that brings the Rankine Cycle working fluid from state 6 to saturations is a shell and tube heat exchanger with 1 shell and 2 tube passes.
- (3) The evaporator section is a fire-tube design, in which the hot exhaust gas from the Brayton cycle flows within the tubes and the water from the Rankine cycle boils on the outside. Pool boiling is assumed and actual heat flux should be well below critical heat flux.
- (4) The superheater, in which the steam of the Rankine cycle is heated from saturation to T_7 operates as a counterflow heat exchanger with two concentric tubes. Steam in the outer annulus and air inside the annulus.
- (5) 200 thin-walled tubes within each heat exchanger section.
- (6) Preheater tubes have a diameter of 20 mm.
- (7) Evaporator and superheater tubes have a diameter of 50 mm.
- (8) Superheater outer tubes have a diameter of 80 mm.
- (9) Preheater baffle spacing is 35% of the shell diameter [10].
- (10) Preheater pitch is 1.5 times the preheater tube diameter [10].
- (11) Preheater has a square tube arrangement because it is a simple, common arrangement [10].

2 Discussion on Environmental Limitations of Cooling Water

The cooling water has environmental regulations affecting it. There are federal guidelines for temperature changes of discharge water compared to the temperature of the water body. For example, the EPA lists the maximum allowable temperature increase of cold water as 5 degrees Fahrenheit [3]. The reason the temperature differences are so low is because discharging much hotter or much colder water can negatively affect the aquatic life within the ocean, lake, river, etc. Because this is a theoretical analysis we can assume a certain time of year when the average water temp is at a desirable temperature. In this case, I chose July because it has higher surface temperatures than other months

3 Schematics and Graphs

3.1 Rankine Cycle. Below are design schematics and diagrams for the Rankine cycle. In the T-S diagram, the entropy is assumed to be equal between states 9-6. Also, the water at state 9 is assumed to be saturated liquid at 40° C meaning the saturation pressure can be found to be 7.384 kPa through interpolation from the steam tables [11].

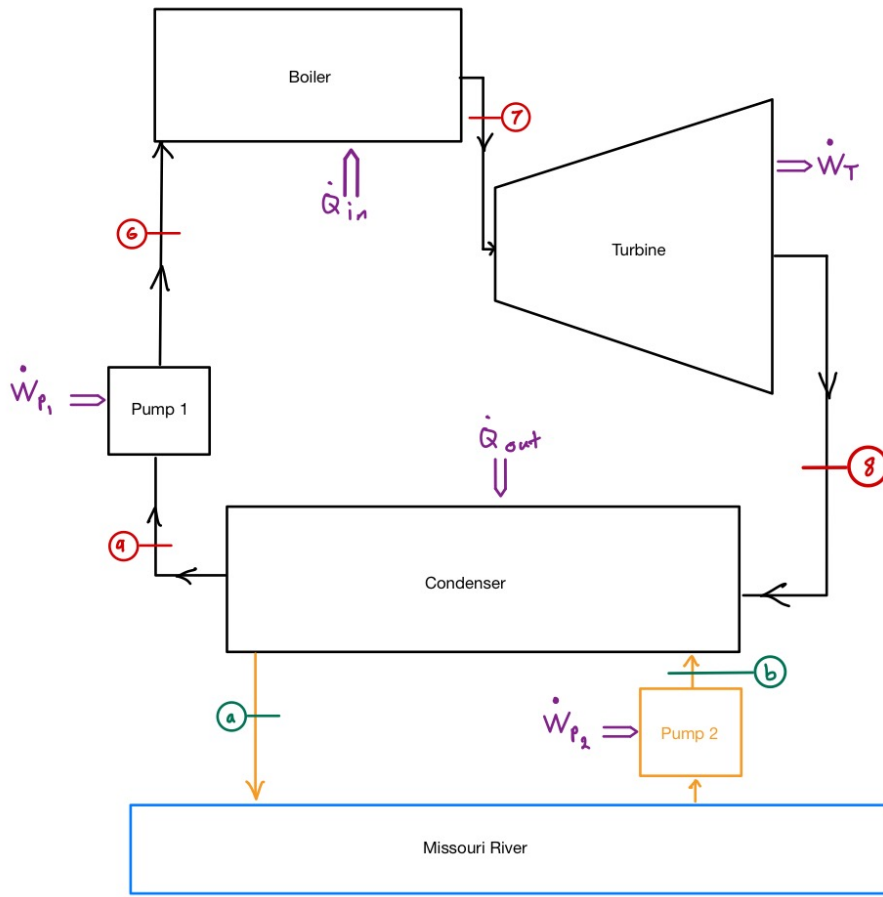


Figure 1 Rankine Cycle schematic including cooling loop.

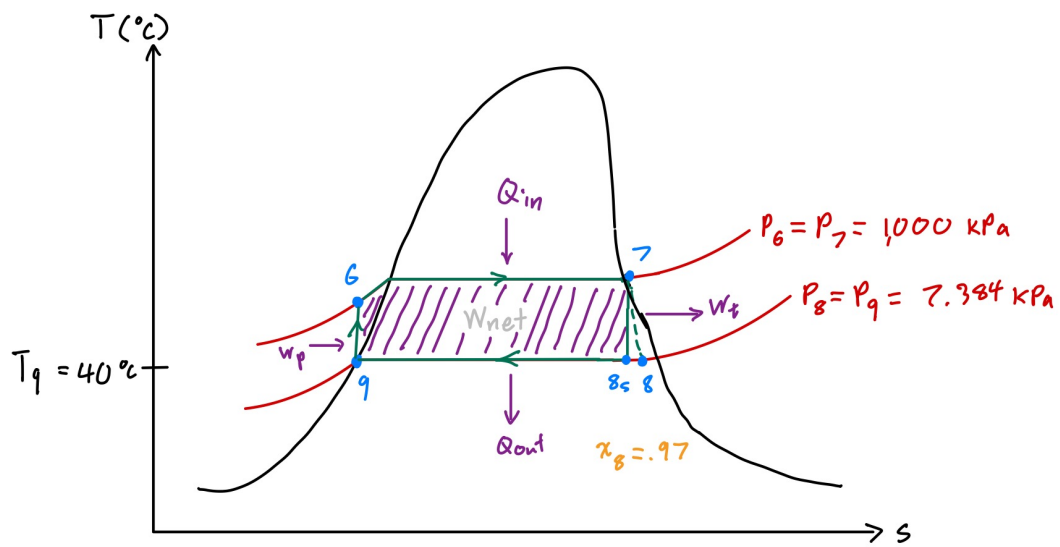


Figure 2 Rankine Cycle T-S diagram.

3.2 Brayton Cycle. Below is a schematic of the Brayton Cycle (the upper cycle of the CCGT diagram) as well as T-S and P- v diagrams for the Brayton Cycle.

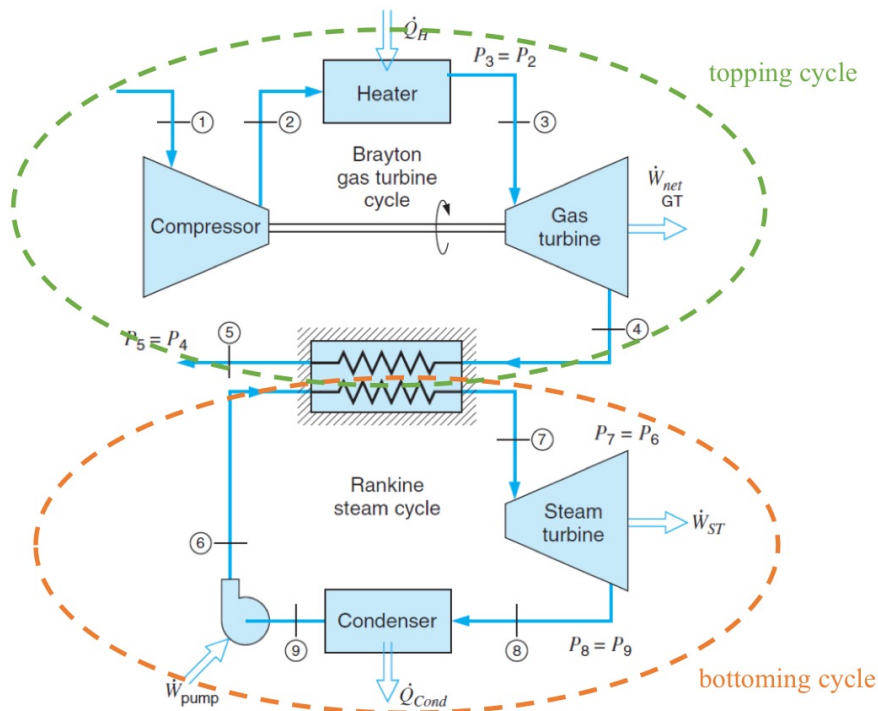


Figure 1: Schematic of a Combined Cycle Gas Turbine (CCGT)

Figure 3 Full CCGT schematic with Brayton as the topping cycle.

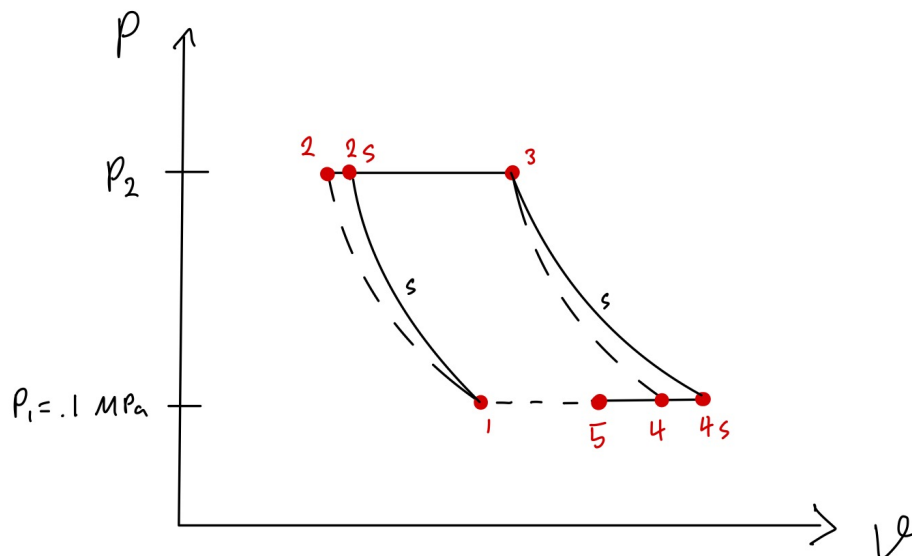


Figure 4 Brayton Cycle P- v diagram.

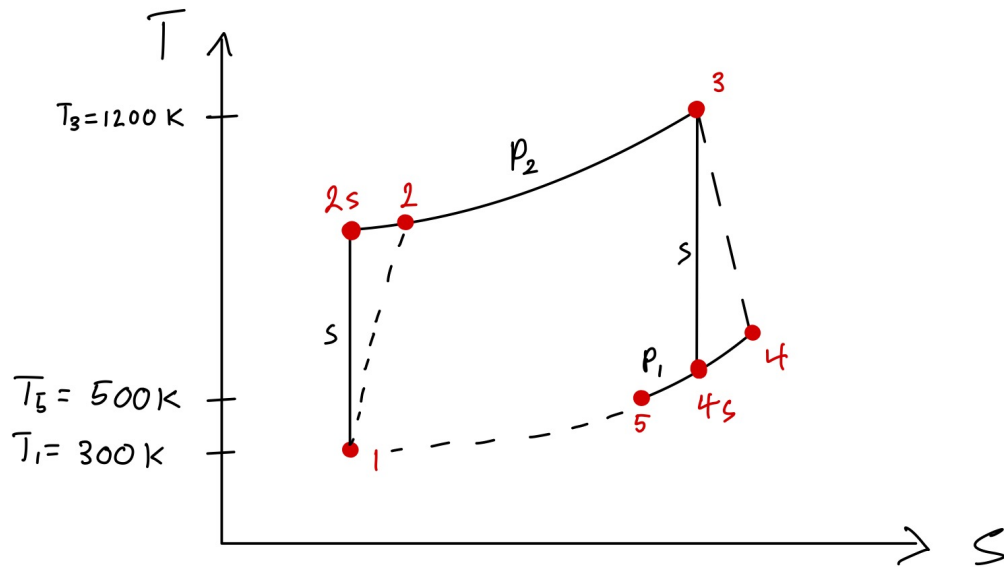


Figure 5 Brayton Cycle T-S diagram.

3.3 Heat Exchangers. Below is a schematic of the general setup of the three heat exchangers as well as T-x diagrams for the different heat exchangers.

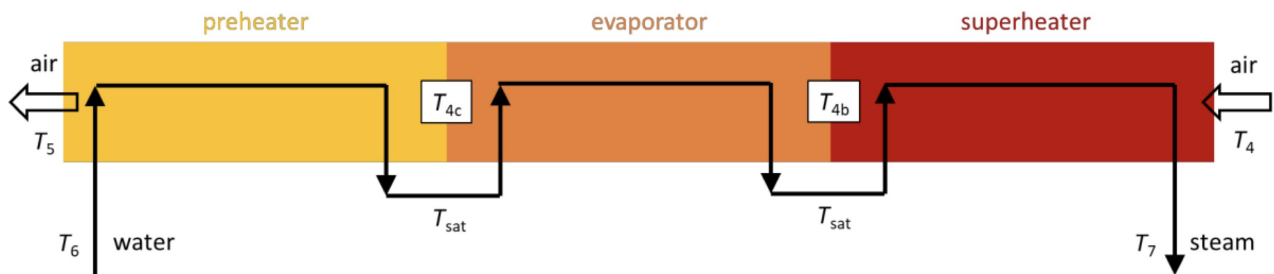


Figure 2: Schematic of the succession of the three heat exchanger sections

Figure 6 Schematic of the three heat exchangers.

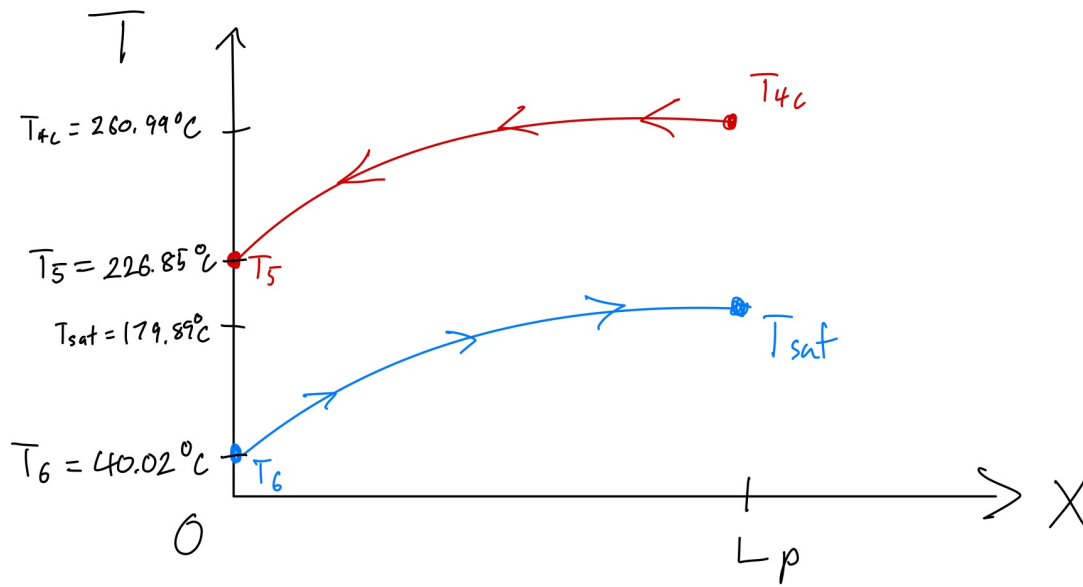


Figure 7 Preheater T-x diagram.

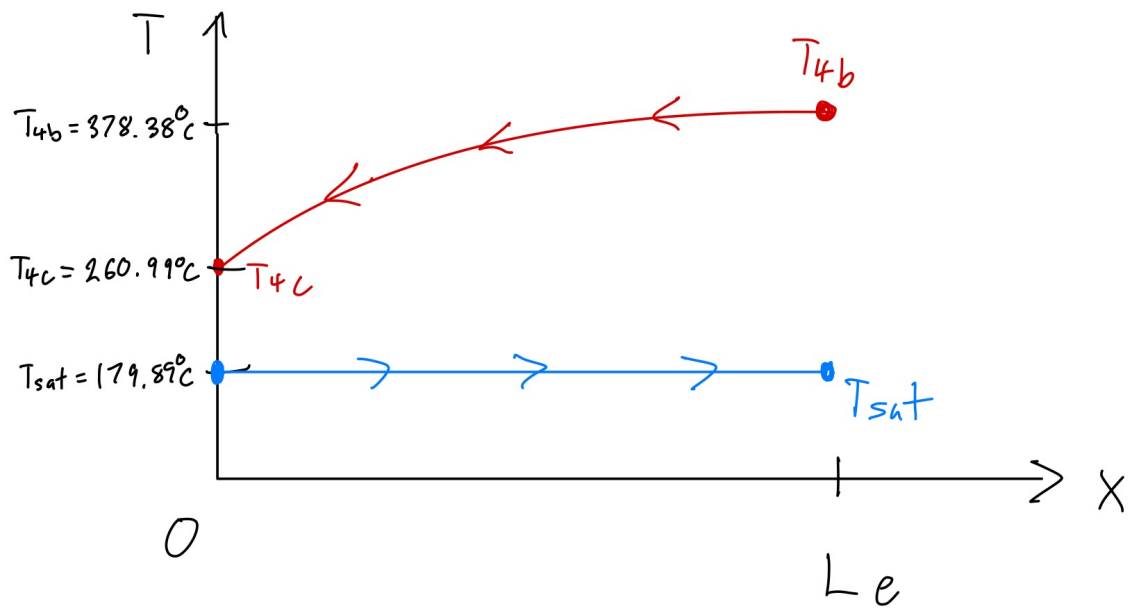


Figure 8 Evaporator T-x diagram.

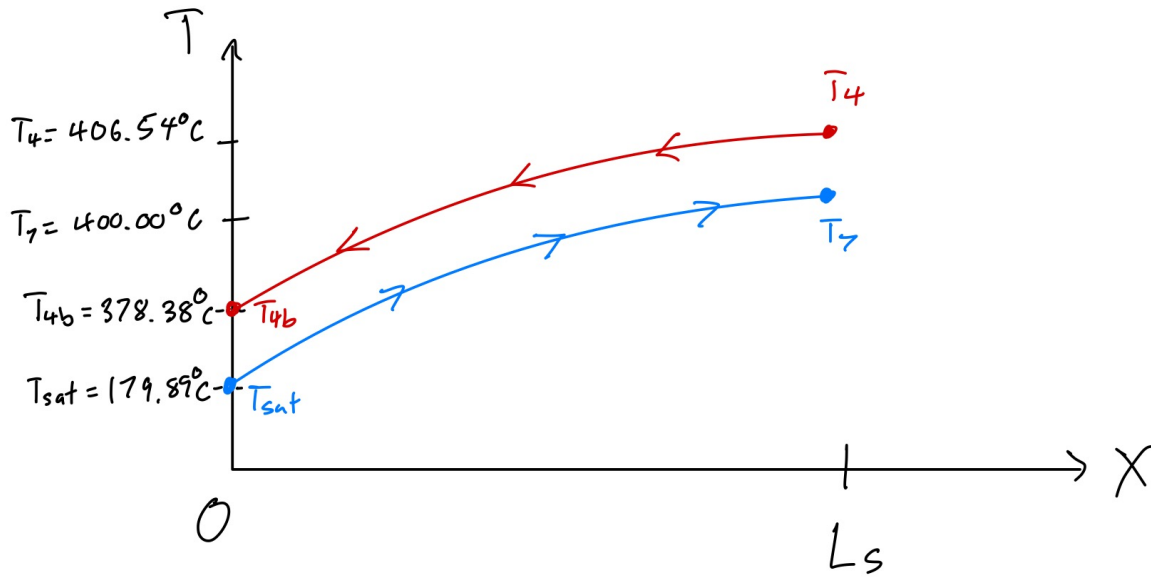


Figure 9 Superheater T-x diagram.

4 Rankine Cycle Calculations and Results

4.1 Rankine Cycle Calculations. Below are the equations that can be used to calculate the efficiency of the closed Rankine cycle.

Solving for the lower temperature bound of the turbine inlet temperature. To find the lower temperature bound for the turbine inlet temperature, one can start by identifying that the pressures for all the states are known. States 9 and 8 have a pressure of 7.384 kPa and states 6 and 7 have a pressure of 1000 kPa. Once this is identified the entropy at state 8 (s_8) can be calculated using the steam tables to find the saturated vapor (s_g) and saturated liquid entropies (s_f) for 7.384 kPa. From these entropies, one can use Equation 1 below to find the entropy for the chosen quality of $x_8 = 88\%$.

$$s_8 = (1 - x_8)s_{8f} + x_8s_{8g} \quad (1)$$

Once the entropy is found, assuming an ideal case, the temperature for the steam turbine can be found using the calculated entropy and known pressure of 1000 kPa. This creates a lower bound because in a non-ideal case, the quality should be higher.

Between State 6 and 7: Boiler. Once the range of temperatures for state 7 has been found, it is now possible to solve for the mass flow rate in the Rankine cycle. To solve for the mass flow rate, one can begin by identifying that enthalpy (h_6) and temperature (T_6) at state 6 can be found from the steam tables using the known pressure of 1000 kPa and the entropy of state 9 where it is saturated liquid at 40° C. It is also possible to find the enthalpy of state 7 (h_7) using the known pressure of 1000 kPa

and the chosen turbine inlet temperature from the defined range. Once these values have been found from the tables, Equation 2 below and the known boundary condition of 30 MW of power being put into the boiler (Q_{in}) can be used to find the mass flow (\dot{m}_r) rate of the Rankine Cycle for the chosen turbine inlet temperature

$$\dot{m}_r = \frac{\dot{Q}_{in}}{(h_7 - h_6)} \quad (2)$$

Between state 7 and 8: Turbine. Once the mass flow rate of the Rankine Cycle has been found, the work flow rate of the turbine (\dot{W}_{tr}) can be calculated. To begin, the entropy of state 7 (s_7) can be found by using the chosen turbine inlet temperature, the known pressure of 1000 kPa, and the assumption that the vapor is superheated. Once s_7 is found the ideal enthalpy at the exit of the turbine (h_{8s}) can be found using s_7 and the known pressure of 7.384 kPa. Once h_{8s} is found, the known h_7 from the mass flow rate calculations and the given boundary condition of a 90% isentropic efficiency ($\eta_{s,t}$) for the turbine can be used with Equation 3 below to find the true enthalpy at state 8 (h_8).

$$\eta_{s,t} = \frac{h_7 - h_8}{h_7 - h_{8s}} \quad (3)$$

Once h_8 is known finding the work flow rate of the turbine is as simple as using the calculated \dot{m}_r , and the calculated h_7 with Equation 4 below.

$$\dot{W}_{tr} = \dot{m}_r(h_7 - h_8) \quad (4)$$

The actual quality of the steam at the outlet of the turbine (x_8) can then be calculated using Equation 5 below

$$h_8 = h_f + x_8 h_{fg} \quad (5)$$

where h_8 is the enthalpy at state 8, h_f is the saturated liquid enthalpy, and h_{fg} is the evaporation enthalpy.

Between state 9 and 6: Rankine Pump. Once \dot{W}_{tr} has been found all that is needed to do an energy balance of the system is the work flow rate of the pump within the Rankine Cycle (\dot{W}_{p1}). Because the \dot{m}_r has already been calculated finding (\dot{W}_{p1}) is as simple as using Equation 6 below with the saturated liquid enthalpy for state 9 (h_9) which can be found from the steam tables as well as h_6 which was found when doing the boiler calculations.

$$\dot{W}_{p1} = \dot{m}_r(h_6 - h_9) \quad (6)$$

Between state 8 and 9: Condenser. Once the work flow rate from the turbine and Pump 1 have been found an energy balance can be used to solve for the power output into the condenser (Q_{out}) because the work input from the boiler was given as a boundary condition of 30 MW. The equation that represents this is Equation 7 below.

$$Q_{out} = Q_{in} + W_{p1} - W_t \quad (7)$$

Once Q_{out} is found the number of tubes in the condenser can be found using heat transfer. To start, Equations 8 and 9 below can be used with the knowledge that $T_9 = T_{sat} = 40^\circ C$ and $T_{coolant,in} = 18.3^\circ C$ $T_{coolant,out} = 21.1^\circ C$.

$$\Delta T_1 = |T_{sat} - T_{coolant,in}| \quad (8)$$

$$\Delta T_2 = |T_{sat} - T_{coolant,out}| \quad (9)$$

Once ΔT_1 and ΔT_2 are known, ΔT_{lm} can be found using Equation 10 below.

$$\Delta T_{lm} = \frac{\Delta T_1 - \Delta T_2}{\ln(\frac{\Delta T_1}{\Delta T_2})} \quad (10)$$

Once ΔT is known, Equations 11 and 12 can be used and rearranged into Equation 13 to find the number of tubes required for the heat exchanger (N). The tube diameter D, tube length L, and heat transfer coefficient of the coolant (U) are given boundary conditions of 25 mm, 10 m, and $U = h_{coolant} = 1000 \frac{W}{m^2 K}$ respectively.

$$Q_{out} = U * A * \Delta T_{lm} \quad (11)$$

$$A = N\pi DL \quad (12)$$

$$N = \frac{Q_{out}}{U\pi LD\Delta T_{lm}} \quad (13)$$

Once the number of tubes needed for the condenser is known, the mass flow rate of the cooling water (\dot{m}_c) can be calculated using Equation 14 where $C_p = 4.18 \frac{J}{g^\circ C}$

$$\dot{m}_c = \frac{Q_{out}}{C_p(T_{coolant,out} - T_{coolant,in})N} \quad (14)$$

Solving for the Major Loss due to friction within the condenser tubes. Once the \dot{m}_c is known the Major Loss due to friction can be calculated. To start, the velocity of the cooling water (V) can be calculated using Equation 15 where density is $\rho = 999 \frac{kg}{m^3}$ and D is the given tube diameter of 25 mm.

$$V = \frac{\dot{m}_c}{\rho \pi \frac{D^2}{2}} \quad (15)$$

Once velocity is calculated, the Reynolds number (Re_D) of the flow can be found using Equation 16 where ρ and D are the same as above and the dynamic viscosity is $\mu = 1.12 * 10^{-3} \frac{N}{ms^2}$.

$$Re_D = \frac{\rho VD}{\mu} \quad (16)$$

Once the Reynolds is known which in all of our inline turbine temperatures is above 4000 it can be concluded that the coolant water flow is turbulent. Knowing that the flow is turbulent, the Moody diagram seen below in Fig. 10 can then be referenced along with the assumed surface roughness of $\epsilon = .0015$ mm for new copper pipes. Assuming the calculated Reynolds number and $\frac{\epsilon}{D}$ ratio are within the Moody chart data, Equation 17 below can then be used to find the friction factor f .

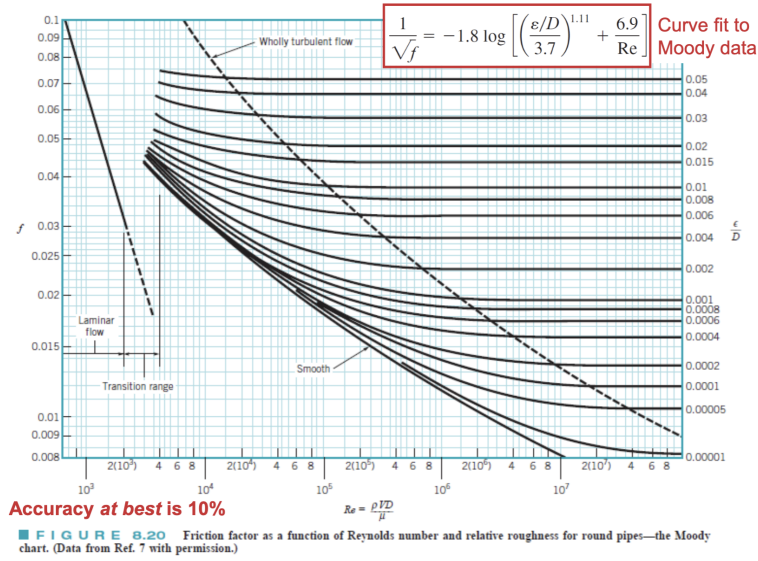


Figure 10 Moody Diagram

$$\frac{1}{\sqrt{f}} = -1.8 \log \left[\left(\frac{\epsilon/D}{3.7} \right)^{1.11} + \frac{6.9}{Re} \right] \quad (17)$$

Once the friction factor is known, the major loss within each pipe can be calculated using Equation 18 below.

$$\text{Major Loss} = f \frac{L}{D} \frac{\rho V^2}{2} \quad (18)$$

Between state a and b: Cooling Pump. Once the major loss within each pipe is known the power required to run the cooling pump can be found. To find it the overall pressure loss from states a to b (from the inlet to the outlet of the condenser) has to be found by multiplying the pressure loss from major losses in each tube by the overall number of tubes as seen in Equation 19.

$$\text{Pressure Loss} = \text{Major Loss} * N \quad (19)$$

Once the overall pressure loss is known the power required for the cooling pump can be found using Equation 20.

$$\dot{W}_{p2} = V \pi \frac{D^2}{2} * \text{Pressure Loss} \quad (20)$$

Overall Rankine Efficiency. Once the power required to run the cooling pump is known, the overall efficiency of the Rankine Cycle ($\eta_{th,r}$) can finally be calculated using Equation 21 below.

$$\eta_{th,r} = \frac{\dot{W}_{p1} + \dot{W}_{p2} - \dot{W}_t}{\dot{Q}_{in}} \quad (21)$$

4.2 Rankine Cycle Results. Based on the code seen below in the Appendix A, the overall Rankine Cycle efficiency as a function of turbine inlet temperature can be seen below in Fig. 11.

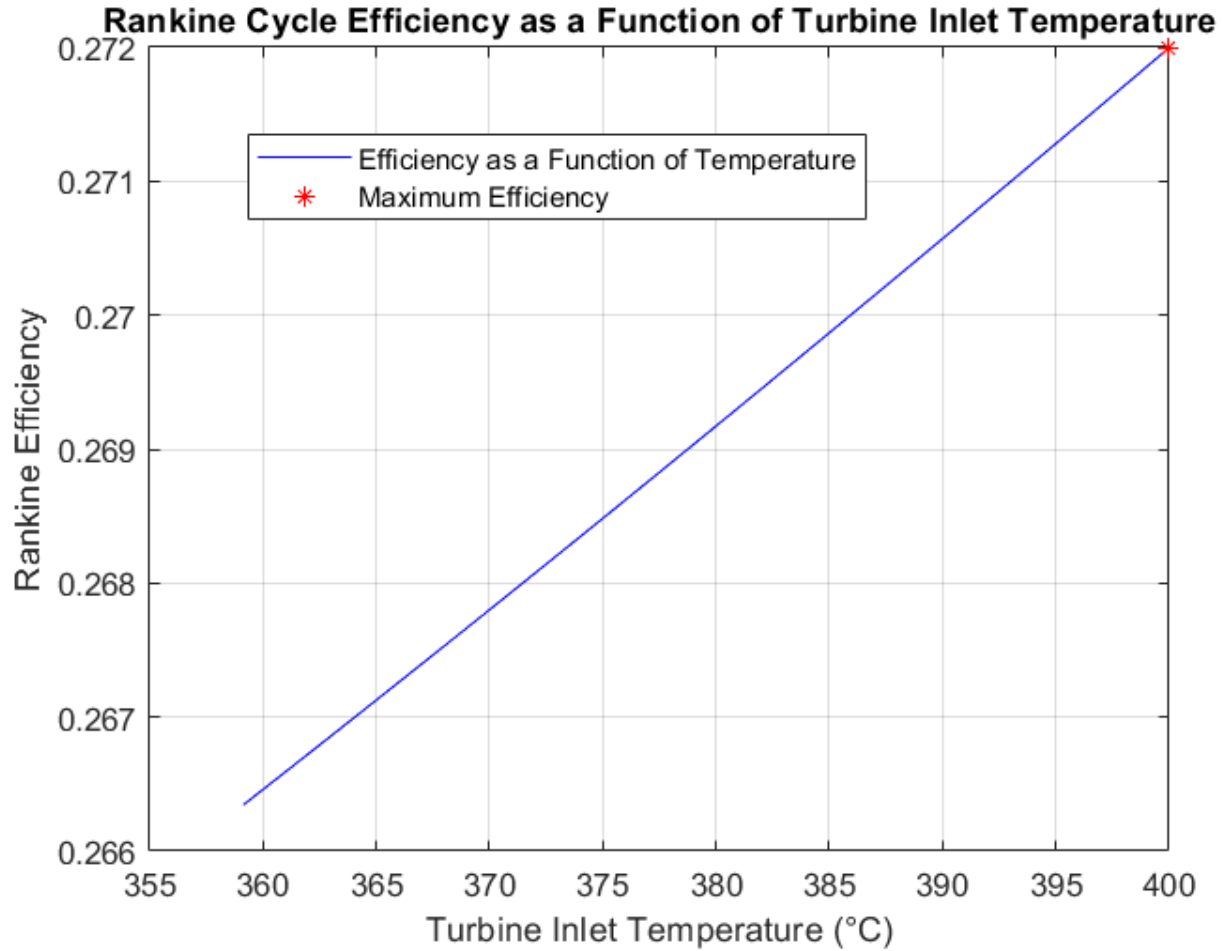


Figure 11 Graph of Rankine Cycle Efficiency as a Function of Turbine Inlet Temperature

The highest efficiency occurs at 400° C with an efficiency of 27.2%.

Some of the other relevant results at this temperature and efficiency are as follows:

- (1) The Rankine Cycle mass flow rate was $9.69 \frac{kg}{s}$.
- (2) The turbine power output was 8.18 MW.
- (3) The power input of the pump within the Rankine cycle was 9.45 kW.
- (4) The power input of the cooling pump was 10.3 kW.
- (5) the number of tubes in the condenser was 1371.39 tubes.
- (6) The turbine exit quality was 88%.

5 Brayton Cycle Calculations and Results

5.1 Brayton Cycle Calculations. Below are the equations that can be used to calculate the efficiency of the open Brayton Cycle and the Solar Tower mirror requirements.

Solving for T_{4s} and T_4 to get \dot{m} for the open Brayton Cycle. In order to find T_4 first T_{4s} needs to be found. This can be done using the polytropic relationships seen in Equation 22 below

$$\frac{T_{4s}}{T_3} = \left(\frac{1}{r_p}\right)^{\frac{k-1}{k}} \quad (22)$$

where T_{4s} is the ideal temperature of the air leaving the turbine [K], T_3 is the temperature of the air entering the turbine [K], r_p is the compression ratio, and k is the heat capacity ratio for air. In this case, because air is treated as an ideal gas $k=1.4$.

Once T_{4s} has been solved T_4 can be found using the isentropic efficiency relationship as seen in Equation 23 below

$$\eta_t = \frac{T_4 - T_3}{T_{4s} - T_3} \quad (23)$$

where η_t is the isentropic efficiency of the turbine, T_4 is the true temperature of the air leaving the turbine [K], and the rest of the variables are the same as above in Equation 22.

Once T_4 has been found one needs to recognize the energy balance across the heat exchanger that is shared with the Rankine cycle. This energy balance can be used to find the mass flow rate of the Brayton Cycle (\dot{m}_b) which can be seen below in Equation 24

$$\dot{m}_b = \frac{Q_L}{C_p(T_4 - T_5)} \quad (24)$$

where Q_L is 30 MW given as a boundary assumption, \dot{m}_b is the mass flow rate found from the heat transfer across the heat exchanger with the Rankine cycle [$\frac{kg}{s}$], C_p is the specific heat of air at 1.004 [$\frac{kJ}{kg-K}$], and the temperatures are the same as above.

Solving for work produced by the turbine W_{tb} in the Brayton cycle. In order to find W_{tb} one simply has to recognize the energy balance across the gas turbine which can be seen below in Equation 25

$$W_{tb} = \dot{m}C_p(T_3 - T_4) \quad (25)$$

where W_t is the work of the turbine [kW], T_3 is the temperature of the air entering the gas turbine given as 1200 K, and the rest of the variables are the same as above.

Solving for T_{2s} and T_2 to get W_c for the compressor. In order to find T_2 first T_{2s} needs to be found. This can be done using the polytropic relationships seen in Equation 26 below

$$\frac{T_{2s}}{T_1} = (r_p)^{\frac{k-1}{k}} \quad (26)$$

where T_{2s} is the ideal temperature of the air leaving the compressor [K], T_1 is the temperature of the air entering the compressor [K], and the rest of the variables are the same as above.

Once T_{2s} has been solved T_2 can be found using the isentropic efficiency relationship as seen in Equation 27 below

$$\eta_c = \frac{T_{2s} - T_1}{T_2 - T_1} \quad (27)$$

where η_c is the isentropic efficiency of the compressor, T_2 is the true temperature of the air leaving the compressor [K], and the rest of the variables are the same as above.

Once T_2 has been found, to find the work of the compressor, one needs to recognize the energy balance across the compressor which can be seen below in Equation 28

$$W_c = \dot{m}_b C_p (T_2 - T_1) \quad (28)$$

where W_c is the work into the compressor [kW], and the rest of the variables are the same as above.

Solving for the thermal energy from the heater Q_h . In order to find Q_H one simply has to recognize the energy balance across the heater which can be seen below in Equation 29

$$Q_h = \dot{m}_b C_p (T_3 - T_2) \quad (29)$$

where Q_H is the thermal energy from the heater [kW], T_3 is the temperature of the air entering the gas turbine given as 1200 K, and T_2 is the solved value from above [K].

Solving for thermal efficiency of the Brayton Cycle $\eta_{th,b}$. To solve for $\eta_{th,b}$ one needs Equation 30 below

$$\eta_{th,b} = \frac{W_{net}}{Q_H} = \frac{W_t - W_c}{Q_H} \quad (30)$$

where the variables are the same as above.

Solving for the number of heliostat mirrors required.. In order to solve for the number of heliostat mirrors required, first all of the above steps need to be completed with literature values of $\eta_c = .88$ and $\eta_t = .93$.

Once this is done the thermal efficiency of the entire system can be graphed with different compression ratios from 5-30 and the highest efficiency can be found. Then the Q_H for the highest efficiency ratio is known and the number of mirrors required can be calculated using Equation 31 below

$$N_h = Q_H \left(\frac{1}{(DNI)} \right) \left(\frac{1}{A} \right) \quad (31)$$

where N_h is the number of mirrors, DNI is the solar irradiance in Kona, HI [$\frac{kW}{m^2}$], and A is the cross-sectional area of a single mirror [m^2].

5.2 Brayton Cycle Results. Based on the Excel sheets seen below in Appendix B, the thermal efficiency of the open Brayton cycle as a function of compression ratio can be seen below in Fig. 12 and the net work of the cycle as a function of compression ratio can be seen in Fig. 13. Note not all possible turbine and compressor efficiency combinations were considered and that the legends indicate turbine/compressor efficiencies.

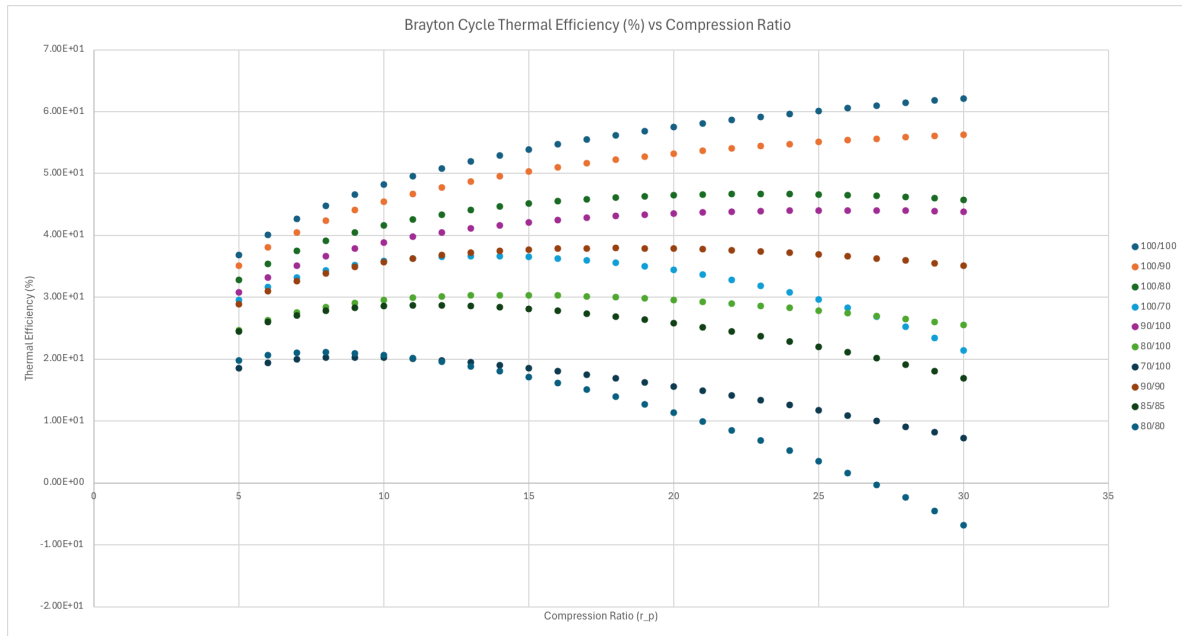


Figure 12 Graph of Brayton cycle efficiency as a function of compression ratio.

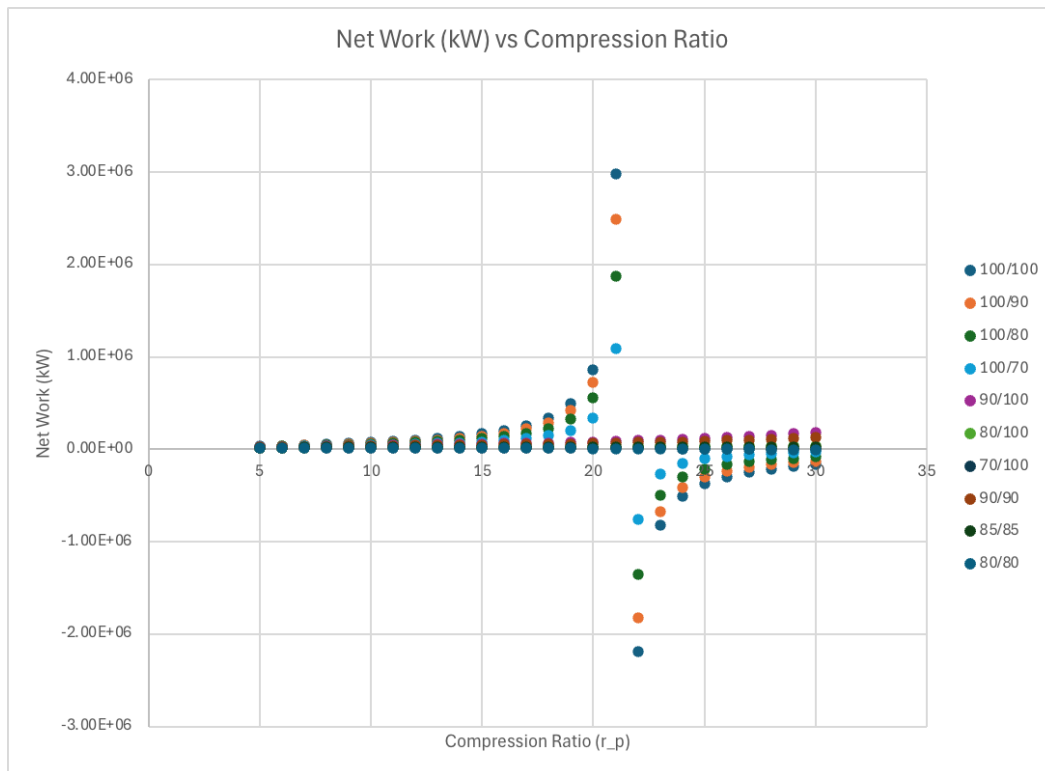


Figure 13 Graph of Brayton cycle net work as a function of compression ratio

Looking at Fig. 12 there is a case where efficiency drops below zero. This case is the 80% turbine efficiency and 80% compressor efficiency. The efficiency dropping below zero, which only happens at the highest compression ratios, simply indicates that the cost to run the compressor became higher than the power output from the turbine. This makes sense because attaining such a high compression ratio would be very expensive, especially with not-as-efficient turbines/compressors.

In terms of Fig. 13 although the majority of the data shows increased net work with an increased compression ratio. It is clear that when the turbine efficiency is 100% there appears a discontinuity in the graph around a compression ratio of 20-22. This happens because with such a high turbine efficiency, T_4 remains the same which in turn leads to a negative \dot{m} when T_4 suddenly becomes higher than the $T_5 = 500K$ given as a boundary. This in turn makes W_{tr} negative which leads to a negative W_{net} . This implies that there is a cutoff for the optimum compression ratio where the thermal efficiency no longer will increase.

Based on Fig. 13 and 12 improvements in turbine efficiency will have a greater effect on improving the overall thermal efficiency and the net power generation. This makes sense because looking at the graphs combinations with a 100% turbine efficiency showed higher thermal efficiencies than combinations with 100% compressor efficiency. Additionally, the net power for combinations with 100% turbine efficiency reached exponential gains at lower compression ratios up to their discontinuities.

Based on the calculations above and the Excel sheet seen in the Appendix B, the Solar Tower graph of efficiency as a function of compression ratio can be seen below in Fig. 14.

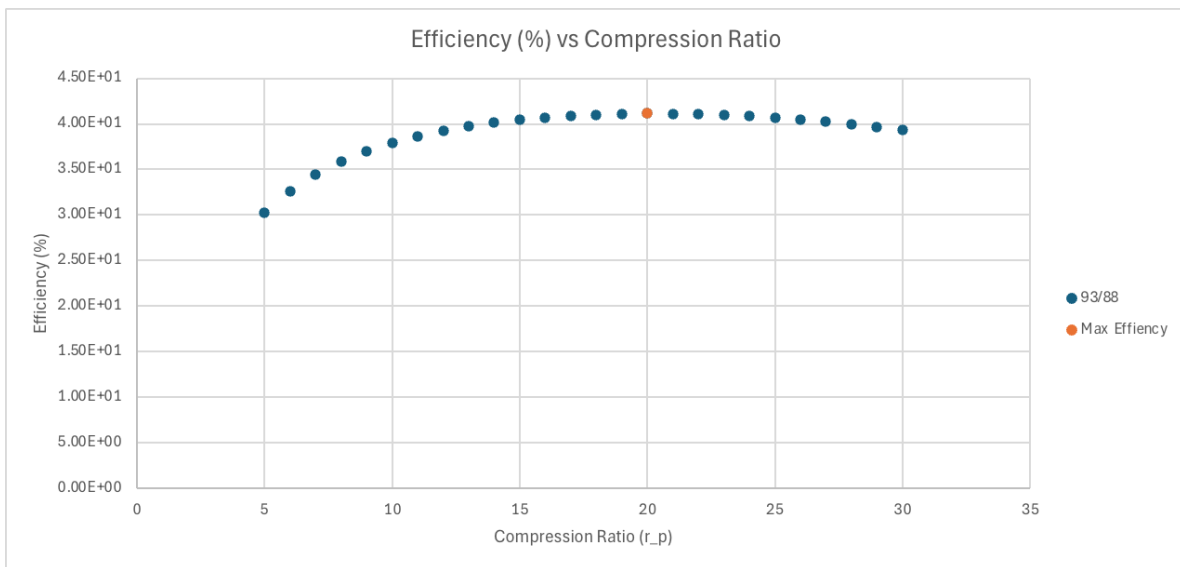


Figure 14 Graph of thermal efficiency as a function of compression ratio.

Using this graph the maximum efficiency for a plant located in Kailua Kona, HI is 41.12% at a compression ratio of 20. Using this efficiency and the Q_H that goes along with it, the number of heliostats required was found to be 17280.

Here is an additional list of final answers garnered from the above work and the Excel file seen in the Appendix B.

- (1) The compressor and turbine efficiencies for the Solar Tower part were 88% and 93% respectively.
- (2) A simple table of results for the various situations can be seen below in Table 1

Table 1 Summary of results.

Combinations	Max Thermal Efficiencies (%)	Compression Ratio	Mass Flow Rate [kg/s]	Net Power Output [kW]	Required Heat Input [kW]	# Heliostats
100/100	62.15	30	-6.51E+02	-1.65E+05	-2.66E+05	-
100/90	56.27	30	-6.51E+02	-1.30E+05	-2.30E+05	-
100/80	46.72	23	-2.97E+03	-4.96E+05	-1.06E+06	-
100/70	36.65	13	3.90E+02	6.26E+04	1.71E+05	-
90/100	44.01	26	6.53E+02	1.27E+05	2.88E+05	-
80/100	30.35	14	1.56E+02	2.67E+04	8.80E+04	-
70/100	20.31	9	9.69E+01	1.26E+04	6.21E+04	-
90/90	37.95	18	3.22E+02	5.78E+04	1.52E+05	-
85/85	28.70	12	1.65E+02	2.54E+04	8.84E+04	-
80/80	21.11	8	1.11E+02	1.40E+04	6.62E+04	-
93/88	41.13	20	5.13E+02	9.30E+04	2.26E+05	17280

6 CCGT Overall Cycle Calculations

Based on the results from the Rankine Cycle and Brayton Cycle separate calculations, a possible setup for the full CCGT can be created. In this case, the Brayton Cycle's highest turbine inlet temperature of 400 ° C was chosen and then a compression ratio that optimizes the efficiency of the realistic Brayton Cycle without going under 400 ° C was deduced. The optimal compression ratio found was 9 at T4=406.54°C using a 93% turbine and 88% compressor efficiency. The plot of this scenario can be seen below in Fig. 15 with a marker indicating the highest efficiency possible while keeping T4 greater than T7=400 ° C.

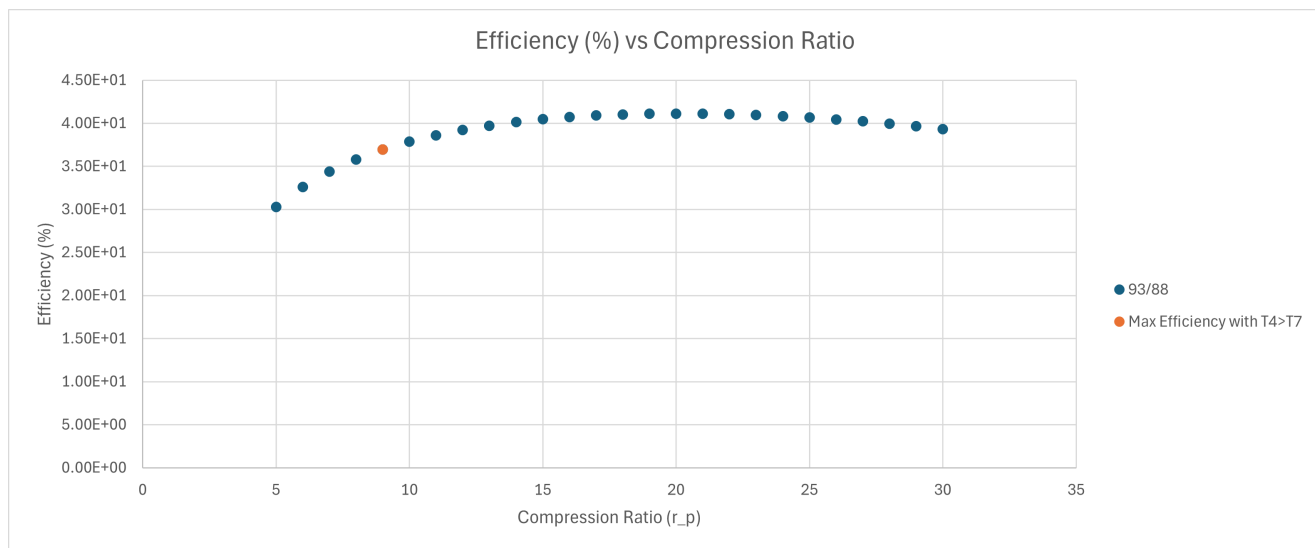


Figure 15 Graph of thermal efficiency as a function of compression ratio with T4 greater than T7 constraint.

Using these input parameters with the calculations for the separate cycles the new combined cycle efficiency can be calculated using Eq. 32.

$$\eta_{th,CCGT} = \frac{W_{net}}{Q_H} = \frac{W_{tr} + W_{tb} - W_{cb} - W_{p1} - W_{p2}}{Q_H} \quad (32)$$

where W_{tr} is the work produced from the turbine in the Rankine cycle, W_{tb} is the work produced from the turbine in the Brayton cycle, W_{cb} is the work consumed by the condenser in the Brayton cycle, W_{p1} is the work consumed by the pump in the Rankine cycle, W_{p2} is the work consumed by the pump sending water to the Rankine cycle, and Q_H is the thermal energy put into the heater in the Brayton cycle. The code for this can be seen below in Appendix C.

The number of heliostats required to produce Q_H for the CCGT parameters can then be calculated using Eq. 31.

7 CCGT Heat Exchanger Calculations

7.1 CCGT Heat Exchanger Heat Transfer/Temperature Equations and Results. The heat transfer from each separate heat exchanger can be calculated. For the preheater, the total heat transfer (Q_p) can be found using Equation 33 below

$$Q_p = \dot{m}_r C_{p,water} (T_6 - T_{sat}) \quad (33)$$

where \dot{m}_r is the known mass flow rate of the water from the Rankine cycle calculations, $C_{p,water}$ is the average specific heat of water between liquid saturation and state 6, T_6 is the temperature at state 6, and T_{sat} is the saturation temperature of the water at 1000 kPa.

For the evaporator, the total heat transfer (Q_e) can be found using Equation 34 below

$$Q_e = \dot{m}_r (h_{sat,vapor} - h_{sat,liquid}) \quad (34)$$

where $h_{sat,liquid}$ is the enthalpy of saturated liquid at 1000 kPa, $h_{sat,vapor}$ is the enthalpy of saturated steam at 1000 kPa, and the other variables are defined previously.

For the superheater, the total heat transfer (Q_s) can be found using Equation 35 below

$$Q_s = \dot{m}_r (h_7 - h_{sat,vapor}) \quad (35)$$

where h_7 is the enthalpy at state 7 and the other variables are previously defined.

The temperatures at each of the points shown along Fig. 6 are either known or can be simply with the calculated Q values from above and the calculated T values from the Rankine and Brayton calculations.

T4, T5, T6, and T7 are all known from the previous calculations done for the Rankine and Brayton cycles separately and are 406.54 °C, 226.85 °C, 40.02 °C, and 400 °C respectively.

T_{sat} can be found using steam tables at 1000 kPa which gives 179.89 ° C. T4b can be found using Equation 36 below

$$T4b = T4 - \frac{Q_s}{\dot{m}_b C_{p,air}} \quad (36)$$

where C_p is the specific heat of air as an ideal gas and all other variables have been defined previously.

T4c can be found using Equation 37 below

$$T4c = T4b - \frac{Q_e}{\dot{m}_b * C_{p,air}} \quad (37)$$

where all variables have been defined previously. The results give $T4b = 378.38$ ° C and $T4c = 260.99$ ° C.

Now that all the temperatures throughout Fig. 6 are known, the heat exchanger tube lengths can be calculated for each section as well as the critical heat flux for the evaporator.

7.2 Heat Exchanger Length and Heat Flux Equations and Results. Below are the separate calculations done for each portion of the heat exchanger. As a reminder, the superheater is a concentric tube counterflow heat exchanger, the evaporator is a fire-tube design, and the preheater is a shell-and-tube design with 1 shell and 2 passes. The code for this can be seen in Appendix D.

Superheater Length Calculations. In order to calculate the heat transfer coefficient of air in the superheater ($h_{air,s}$) the mean air velocity, the Reynolds number and the Nusselt number for the air have to be calculated. The mean air velocity ($V_{m,air,s}$) can be calculated using Equation 38 below

$$V_{m,air,s} = \frac{\dot{m}_b}{\rho_{air} \pi N \left(\frac{D_i}{2}\right)^2} \quad (38)$$

where \dot{m}_b is the mass flow rate of air from the Brayton cycle, ρ_{air} is the density of air as an ideal gas, N is the number of tubes, and D_i is the diameter of the inner superheater tube given as 50 mm.

Once, the mean air velocity has been found, the Reynolds number for air in the superheater ($Re_{air,s}$) can be found using Equation 39 below

$$Re_{air,s} = \frac{\rho_{air} V_{m,air,s} D_i}{\mu_{air}} \quad (39)$$

where μ_{air} is the dynamic viscosity of air as an ideal gas and the other variables are defined above.

After finding $Re_{air,s}$ the Nusselt number for air in the superheater ($Nu_{air,s}$) can be found using Equation 40 below

$$Nu_{air,s} = .023 Re_{air,s}^{4/5} Pr_{air}^4 \quad (40)$$

where Pr_{air} is the Prandtl number of air as an ideal gas and the other variable is defined above.

Once $Nu_{air,s}$ has been found $h_{air,s}$ can be found using Equation 41 below

$$h_{air,s} = \frac{Nu_{air,s} k_{air}}{D_i} \quad (41)$$

where k_{air} is the thermal conductivity of air as an ideal gas and the other variables are defined above.

Once $h_{air,s}$ has been found the heat transfer coefficient for the superheated water vapor in the superheater ($h_{vapor,s}$). Again the mean velocity, the Reynolds number, and the Nusselt number for the vapor have to be calculated. The mean velocity ($V_{m,vapor,s}$) can be calculated using Equation 42 below

$$V_{m,vapor,s} = \frac{\dot{m}_r}{\rho_{vapor,s} \pi N ((\frac{D_o}{2})^2 - (\frac{D_i}{2})^2)} \quad (42)$$

where \dot{m}_r is the mass flow rate from the Rankine cycle, $\rho_{vapor,s}$ is the average density of the vapor between saturation and state 7, D_o is the outer diameter of the superheater tubes given as 80mm, and the other variables are defined above.

Once $V_{m,vapor,s}$ has been found the Reynolds can be found using Equation ?? below

$$Re_{vapor,s} = \frac{\rho_{vapor,s} V_{m,vapor,s} D_h}{\mu_{vapor,s}} \quad (43)$$

where $\mu_{vapor,s}$ is the average dynamic viscosity of the vapor between saturation and state 7 [], D_h is the hydraulic diameter defined in Equation 44 below, and the other variables are defined above.

$$D_h = D_o - D_i \quad (44)$$

After finding $Re_{vapor,s}$, the Nusselt number for the vapor ($Nu_{vapor,s}$) can be found using Equation 45 below

$$Nu_{vapor,s} = .023 Re_{vapor,s}^{4/5} Pr_{vapor,s}^{.3} \quad (45)$$

where $Pr_{vapor,s}$ is the average Prandtl number of the vapor between saturation and state 7 [12] and the other variables are defined above.

$h_{vapor,s}$ can be calculated after finding $Nu_{vapor,s}$ using Equation 46 below

$$h_{vapor,s} = \frac{Nu_{vapor,s} k_{vapor,s}}{D_h} \quad (46)$$

where $k_{vapor,s}$ is the average thermal conductivity of the vapor between saturation and state 7 [], and the other variables are defined above.

After finding the heat transfer coefficient for the air and the vapor in the superheater, the overall heat transfer coefficient for the superheater (U_s) can be found using Equation 47 below.

$$U_s = \left(\frac{1}{h_{air,s}} + \frac{1}{h_{vapor,s}} \right)^{-1} \quad (47)$$

Before solving for the superheater tube length, the log mean temperature difference (LMTD) of the superheater ($\Delta_{LMTD,s}$) still needs to be calculated. The LMTD can be calculated using Equation 48 below

$$\Delta_{LMTD,s} = \frac{\Delta_{T1,s} - \Delta_{T2,s}}{\ln\left(\frac{\Delta_{T1,s}}{\Delta_{T2,s}}\right)} \quad (48)$$

where $\Delta_{T1,s}$ is the difference between the hot inlet ($T4b$) and cold outlet (T_{sat}) temperatures of the superheater as seen in Equation 49 and $\Delta_{T2,s}$ is the difference between the hot outlet ($T4$) and cold inlet ($T7$) temperatures of the superheater as seen in Equation 50.

$$\Delta_{T1,s} = T4b - T_{sat} \quad (49)$$

$$\Delta_{T2,s} = T4 - T7 \quad (50)$$

Finally once $\Delta_{LMTD,s}$ has been calculated, the length of the superheater tubes can be calculated using Equation 51 below

$$L_s = \frac{Q_s}{U_s \Delta_{LMTD,s} N \pi D_i} \quad (51)$$

where Q_s is the heat transfer for the superheater calculated from Section 7.1, and the other variables have been defined above.

Evaporator Length and Heat Flux Calculations. To find the length of the evaporator tubes, a similar process to the superheater is conducted. The difference is that for the evaporator, the heat transfer coefficient of the water/vapor does not need to be accounted for in the overall heat transfer coefficient (U_e) because of the pool boiling and phase change that occurs. Because of the phase change, the heat transfer coefficient for the water approaches infinity which means it essentially adds nothing to U_e [13].

Because the diameter of the tubes through which the air travels (D) remains the same, the Reynolds number ($Re_{air,e}$), Nusselt number ($Nu_{air,e}$), and heat transfer coefficient ($h_{air,e}$) of the air in the evaporator are the same as in the superheater as seen in Equations 52, 53, and 54.

$$Re_{air,e} = Re_{air,s} \quad (52)$$

$$Nu_{air,e} = Nu_{air,s} \quad (53)$$

$$h_{air,e} = h_{air,s} \quad (54)$$

U_e can thus be calculated using Equation 55 below.

$$U_e = \left(\frac{1}{h_{air,e}}\right)^{-1} \quad (55)$$

Again similar to the superheater, the LMTD for the evaporator ($\Delta_{LMTD,e}$) can be calculated using Equation 56 below

$$\Delta_{LMTD,e} = \frac{\Delta_{T1,e} - \Delta_{T2,e}}{\ln\left(\frac{\Delta_{T1,e}}{\Delta_{T2,e}}\right)} \quad (56)$$

where $\Delta_{T1,e}$ is the difference between the hot inlet ($T4c$) and cold outlet (T_{sat}) temperatures of the evaporator as seen in Equation 57 and $\Delta_{T2,e}$ is the difference between the hot outlet ($T4b$) and cold inlet (T_{sat}) temperatures of the evaporator as seen in Equation 58.

$$\Delta_{T1,e} = T4c - T_{sat} \quad (57)$$

$$\Delta_{T2,e} = T4b - T_{sat} \quad (58)$$

The length of the evaporator tubes (L_e) can then be calculated using Equation 59 below

$$L_e = \frac{Q_e}{U_e \Delta_{LM,e} N \pi D} \quad (59)$$

where Q_e is the heat transfer from the evaporator calculated in Section 7.1 and the other variables are defined above.

In addition to the length of the evaporator, another variable that has to be calculated is the heat flux. The heat flux needs to be calculated to make sure it stays under the critical heat flux (q''_{CHF}) and thus the pool boiling is still an effective form of heat transfer [13]. The heat flux of the evaporator (q'') can be calculated using Equation 60 below

$$q'' = \frac{Q_e}{N \pi D L_e} \quad (60)$$

where the variables have all been defined above.

The critical heat flux of the evaporator can be calculated using Equation 61 below

$$q''_{CHF} = C_z h_{fg} \rho_v \left(\frac{\sigma_{lv} g (\rho_l - \rho_v)}{\rho_v^2} \right)^{\frac{1}{4}} \quad (61)$$

where C_{zh} is the Zuber constant of .131 for cylinders, h_{fg} is the enthalpy at vaporization for air as an ideal gas, ρ_v is the saturated vapor density of air as an ideal gas, ρ_l is the saturated liquid density of air as an ideal gas, σ_{lv} is the surface tension, and g is gravity.

Preheater Length Calculations. To find the length of the preheater tubes a different approach has to be taken than for the evaporator or superheater. Instead of using the LMTD method the epsilon-NTU method has to be used.

To begin the epsilon-NTU method, the effectiveness (ϵ) first has to be calculated using Equation 62 below

$$\epsilon = \frac{Q_p}{Q_{p,max}} \quad (62)$$

where Q_p is the heat transfer across the preheater calculated in Section 7.1, and $Q_{p,max}$ is the maximum possible heat transfer for the preheater. $Q_{p,max}$ can be calculated using Equation 63 below

$$Q_{p,max} = C_{p,water} \dot{m}_r (T4c - T6) \quad (63)$$

where $C_{p,water}$ is the minimum heat capacity of the system which in this case is the average between liquid saturation and state 6 of the water, T_{4c} is the hot inlet temperature of the air, T_6 is the cold inlet temperature of the water, and the other variables are defined above.

Once ϵ has been calculated the parameter E can be calculated using Equation 64 below

$$E = \frac{\left(\frac{2}{\epsilon}\right) - (1 + C_r)}{(1 + C_r)^{\frac{1}{2}}} \quad (64)$$

where C_r is the heat capacity rate of the system, and the other variables are defined above. C_r can be defined as Equation 65 below

$$C_r = \frac{C_{p,water}\dot{m}_r}{C_{p,air}\dot{m}_b} \quad (65)$$

where $C_{p,water}$ is the average specific heat of the water between liquid saturation and state 6, $C_{p,air}$ is the specific heat of air as an ideal gas, and the other variables are defined previously.

After finding the parameter E and ϵ , the NTU for the evaporator (NTU) can be calculated using Equation 66 below

$$NTU = -(1 + C_r^2)^{-\frac{1}{2}} \ln\left(\frac{E - 1}{E + 1}\right) \quad (66)$$

where all variables have been defined previously.

Once the epsilon-NTU relations have been solved, the overall heat transfer coefficient of the preheater (U_p) still has to be solved.

Before solving for U_p the Reynolds, Nusselt, heat transfer coefficient of both the air and water need to be found where air is in the shell and water in the tubes. To begin finding the heat transfer coefficient for the air in the preheater ($h_{air,p}$), first the shell diameter has to be calculated. The shell diameter can be calculated by observation knowing that there are 400 tubes in a square design to fit within the shell. Thus a setup of 20 tubes by 20 tubes must fit into the diameter with a pitch of 1.5 times the tube diameters and a baffle spacing of 35% the shell diameter. The side length of a square that would fit this setup (S_L) can be calculated using Equation 67 below

$$S_L = (19S_D) + D_p \quad (67)$$

where S_D is the tube-tube pitch distance and D_p is the diameter of the preheater tubes given as 20 mm.

Once the side length is known, the required shell diameter (D_{shell}) can be easily calculated using the Pythagorean theorem as seen below in Equation 68 below

$$D_{shell} = \sqrt{S_L^2 + S_L^2} \quad (68)$$

After calculating the shell diameter the shell-side effective crossflow area (S_m) can be calculated using Equation 69 below

$$S_m = b_s(S_D - D_p) \quad (69)$$

where b_s is the baffle spacing of .35 times the shell diameter and the other variables are previously defined.

The shell-side mass flow rate (G_s) can be calculated using Equation 70 below

$$G_s = \frac{\dot{m}_b}{S_m} \quad (70)$$

where all variables have been previously defined.

After finding G_s the equivalent diameter of the shell with the tubes (D_e) can be calculated using Equation 71 below

$$D_e = \frac{4(C_{p,D_p} S_d^2 - \frac{\pi D_p^2}{4})}{\pi D_p} \quad (71)$$

where C_{p,D_p} is a configuration constant which is 1 for a square pitch setup and all other variables have been previously defined.

Finally, the Reynolds number for the air in the shell of the preheater ($Re_{s,air,p}$) can be calculated using Equation 72 below

$$Re_{s,air,p} = \frac{D_e G_s}{\mu_{air}} \quad (72)$$

where all variables are defined previously.

The Nusselt number for the air in the shell ($Nu_{air,p}$) of the preheater can be calculated using Equation 73

$$Nu_{air,p} = .36 Re_{s,air,p}^{.55} Pr_{air}^{\frac{1}{3}} \quad (73)$$

where all the variables have been defined previously.

The heat transfer coefficient of the air in the preheater ($h_{air,p}$) can then be calculated using Equation 74

$$h_{air,p} = \frac{k_{air} Nu_{air,p}}{D_p} \quad (74)$$

where all variables have been defined previously.

The Reynolds number of the water in the preheater ($Re_{water,p}$) can be calculated in a much easier fashion than for the air using Equation 75 below

$$Re_{water,p} = \frac{4\dot{m}_r}{\pi D_p \mu_{s,water,p} N} \quad (75)$$

where $\mu_{s,water,p}$ is the average dynamic viscosity of the water between state 6 and the saturation temperature and all other variables have been defined previously.

To find the Nusselt number of the water in the preheater ($Nu_{water,p}$) Equation 76 below can be used

$$Nu_{water,p} = .023 Re_{water,p}^{\frac{4}{5}} Pr_{water,p}^{.4} \quad (76)$$

where $Pr_{water,p}$ is the average Prandtl number of water between state 6 and saturation temperature and all other variables have been defined previously.

The heat transfer coefficient of the water in the preheater ($h_{water,p}$) can then be calculated using Equation 77 below

$$h_{water,p} = \frac{Nu_{water,p} k_{water,p}}{D_p} \quad (77)$$

where $k_{water,p}$ is the average thermal conductivity of the water between state 6 and saturation temperature and all other variables are previously defined.

Once $h_{air,p}$ and $h_{water,p}$ have both been calculated the overall heat transfer coefficient of the preheater (U_p) can be calculated using Equation 78 below

$$U_p = \left(\frac{1}{h_{air,p}} + \frac{1}{h_{water,p}} \right)^{-1} \quad (78)$$

where all variables have been previously defined.

Finally, the length of the preheater tubes (L_p) can be calculated using Equation 79 below

$$L_p = \frac{NTUC_{water,p} \dot{m}_r}{U_p \pi D_p N} \quad (79)$$

where all variables have been previously defined.

8 Final Results Summary and Sanity Check

8.1 CCGT Results Summary. The optimized plots for the CCGT although already seen above in this report are reiterated below. The Rankine cycle has an optimized state at $T7 = 400^\circ\text{C}$ and an efficiency of 27.2%. The Brayton Cycle has an optimized state at a compression ratio of 9, $T4 = 406.54^\circ\text{C}$, and efficiency of 37% because of the constraint that $T4$ be greater than $T7$.

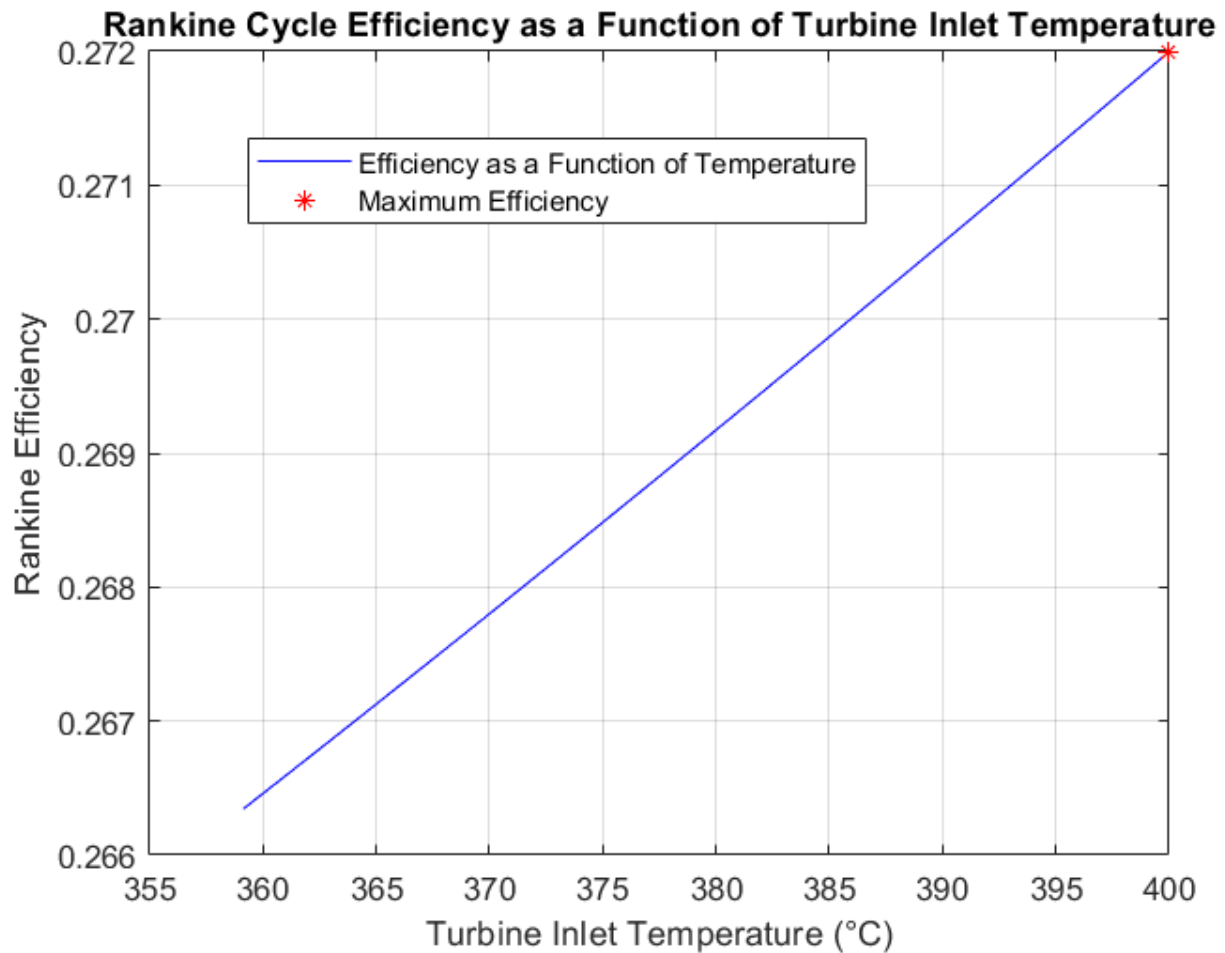


Figure 16 Graph of Rankine Cycle Efficiency as a Function of Turbine Inlet Temperature

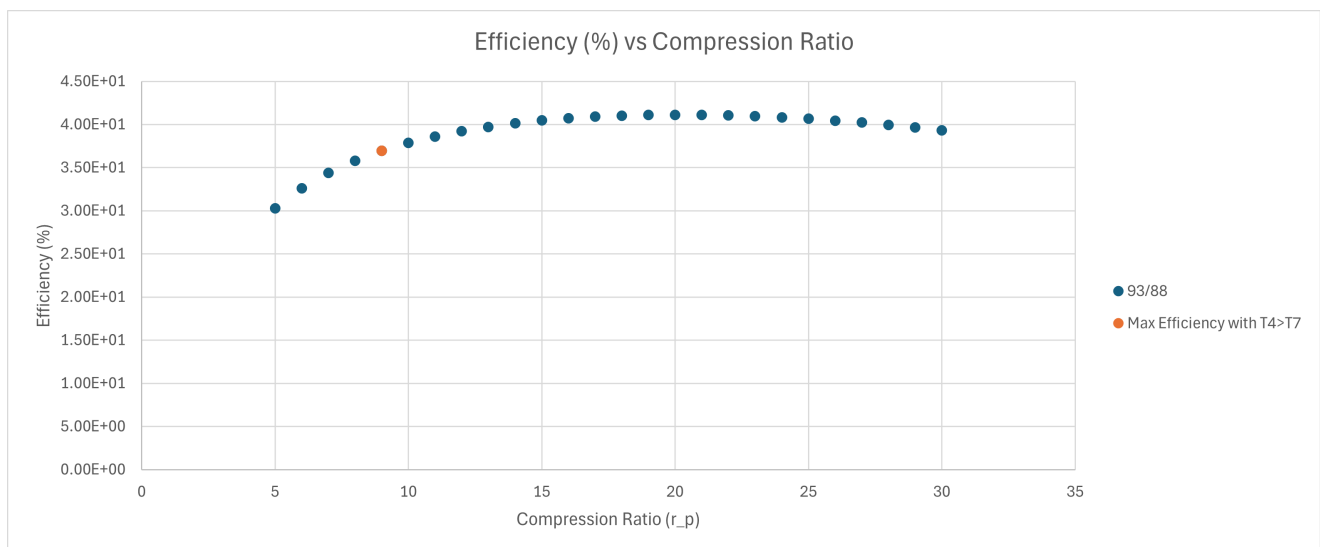


Figure 17 Graph of thermal efficiency as a function of compression ratio with T₄ greater than T₇ constraint.

Below in Table 2 is a summary of the final answers as requested.

Table 2 Summary of Final Results

Variable	Value	Unit
Turbine Inlet Temperature	400	C
Turbine Outlet Quality	92	%
Rankine Thermodynamic Efficiency	27.2	%
Rankine Mass Flow Rate	969	kg/s
Brayton Compression Ratio	9	-
Brayton Heat Input	101	MW
Brayton Thermodynamic Efficiency	37	%
Brayton Mass Flow Rate	167	kg/s
CCGT Number of Heliostats	7,685	-
CCGT Thermodynamic Efficiency	45.1	%
CCGT Net Power Output	45.3	MW
Superheater Tube Length	31.2	m
Evaporator Tube Length	8.4	m
Preheater Tube Length	3.4	m
Pitch	1.5 X Tube Diameter	-
Arrangement	Square	-
Shell Diameter	0.83	m
Baffle Spacing	35	% of Shell Diameter
Evaporator Actual Heat Flux	74	kW/m ²
Evaporator Critical Heat Flux	2,629	kW/m ²

8.2 Heat Exchanger Sanity Check. A simple sanity check for the heat exchanger calculations is simply adding up the separate heat transfer from each of the sections in order to verify that it is the 30 MW it is supposed to be from the given boundary conditions. In our case we got a preheater value of $Q_p = 5.97MW$, an evaporator value of $Q_e = 19.52MW$, and a superheater value of $Q_s = 4.72MW$. This adds up to $Q_{total} = 30.21MW$ which is a solid indication that our heat transfer values for the exchangers are correct. In terms of the length calculations, a good way to check them is by simply comparing them to expected values in literature. For the preheater according to one source standard lengths for shell and tube exchangers are anywhere from 8-12 ft with 3/4 to 1 in tube diameters[10]. In our results we got a length of 3.4 m (about 11.4 ft) and a tube diameter of 20 mm (about .79 in) indicating relatively close results. For the evaporator according to one source reasonable length for a fire tube boiler is 6 m [14]. For the superheater, because the same calculation method was employed as for the evaporator and its values were close to literature values it is reasonable to conclude that the length value found of 31.2 m is accurate. The preheater values may not be perfect because the Reynolds number found for the air is on the order of 10^7 which is outside of the given range for the

Kern Method Nusselt-Reynolds correlation used which maxes at 10^6 . Additionally the superheater length may be higher than usual. This is because the difference between T4 and T7 is only about 6°C even though it should have been on the order of a few tens.

8.3 CCGT Sanity Check. A simple sanity check for the overall cycle is to first check the Rankine Cycle efficiency in comparison to literature. According to literature the Rankine Cycle efficiency is around 30% which is close to the found value of 27.2% [15, 16]. The calculated answer is slightly below the expected 30% but the literature articles have slightly different setups such as a waste heat recovery and a higher isentropic turbine efficiency [15, 16]. Once we add on the Brayton cycle as the topping cycle, we would expect the overall thermal efficiency to increase because the Rankine cycle is using the waste heat from the Brayton Cycle to increase the overall net power. In the case of this paper, an overall efficiency of 45.1% was found. Literature puts the expected values of the overall cycle anywhere from 50-60% [17]. This means that our value is slightly lower than expected but arguably still within the range of reason. In terms of a sanity check for the solar tower calculations, a literature review found that for a solar tower plant with a thermal input of 136 MW, DNI of $850 \frac{\text{W}}{\text{m}^2}$, and heliostat efficiency of 57% the square meters of the heliostat field was 302,449 m^2 [18]. In comparison, our example found a 768500 m^2 field would bring in 101 MW with a DNI of $130.8 \frac{\text{W}}{\text{m}^2}$ assuming perfect solar to thermal energy conversion. This makes sense considering our area is about 2.7 times the literature study, the literature power output is about 1.3 times greater, the literature DNI is 6.5 times greater, and the literature efficiency is about half. Obviously this is not a perfect comparison but shows the heliostat range is ballpark what can be seen in literature.

References

- [1] Kumana, J. D., 2018, “Essentials of Steam Turbine Design and Analysis,” accessed Feb. 6, 2024, <https://www.aidc.org/resources/publications/cep/2018/august/essentials-steam-turbine-design-and-analysis#:~:text=Steam%20turbines%20typically%20rotate%20at,steam%20quality%20of%2097%25>.
- [2] 2023, “Missouri River bl Holter Dam nr Wolf Cr Mt,” USGS, accessed Feb. 6, 2024, <https://waterdata.usgs.gov/monitoring-location/06066500/#parameterCode=00010&period=P365D&showMedian=false>
- [3] 1980, “Water Quality Standards Criteria Digest A Compilation of State/Federal Criteria,” Environmental Protection Agency Office of Water Regulations and Standards, accessed Feb. 6, 2024, <https://nepis.epa.gov/Exe/ZyNET.exe/2000YTVI.TXT?ZyActionD=ZyDocument&Client=EPA&Index=1976+Thru+1980&Docs=&Query=&Time=&EndTime=&SearchMethod=1&TocRestrict=n&Toc=&TocEntry=&QField=&QFieldYear=&QFieldMonth=&QFieldDay=&IntQFieldOp=0&ExtQFieldOp=0&XmlQuery=&File=D%3A%5Czyfiles%5CIndex%20Data%5C76thru80%5Ctxt%5C00000008%5C2000YTVI.txt&User=ANONYMOUS&Password=anonymous&SortMethod=h%7C-&MaximumDocuments=1&FuzzyDegree=0&ImageQuality=r75g8/r75g8/x150y150g16/i425&Display=hpfr&DefSeekPage=x&SearchBack=ZyActionL&Back=ZyActionS&BackDesc=Results%20page&MaximumPages=1&ZyEntry=1&SeekPage=x&ZyPURL>
- [4] 2004, “Condensing Temperature Clues,” The Air Conditioning News, accessed Feb. 6, 2024, <https://www.achnews.com/articles/91476-condensing-temperature-clues#:~:text=Condenser%20splits%20can%20range%20from,the%20condenser%20split%20will%20be>.
- [5] 2020, “CTech Tip: Temperature changes on a condenser,” Ritchie Engineering Co., accessed Feb. 6, 2024, <https://www.fleetmaintenance.com/tech-tips/blog/21140063/ritchie-engineering-co-tech-tip-temperature-changes-on-a-condenser>
- [6] 2001, “The commonly used material for condenser tubes,” World Iron Steel, accessed Feb. 6, 2024, <https://www.wildsteel.com/the-commonly-used-material-for-condenser-tubes/>
- [7] 2003, “Roughness and Surface Coefficients,” The Engineering ToolBox, accessed Feb. 6, 2024, https://www.engineeringtoolbox.com/surface-roughness-ventilation-ducts-d_209.html
- [8] 2023, “Solar Energy in 96740 (Kailua Kona, HI),” Solar Energy Local, accessed March 3, 2024, <https://www.solarenergylocal.com/states/hawaii/96740/#:~:text=Solar%20Radiation%20Analysis%20for%2096740&text=The%20three%20months%20that%20historically,3.22%20kWh%20Fm2%20Fday>.
- [9] Sarkar, J., 2010, “Thermodynamic analyses and optimization of a recompression N2O Brayton power cycle,” accessed March 3, 2024, https://www.sciencedirect.com/science/article/pii/S0360544210002422?casa_token=Ptvx2O8QtX4AAAAA:iU9hIPwwJOOzm75uPOiwq0oRGq0ymonk3unELPerhKUqG0wnNOMKgaBW-3-y10Yc6EF3tb64w
- [10] 2020, “Heat Exchangers,” The University of Oklahoma, accessed Apr. 1, 2024, <https://www.ou.edu/class/che-design/design%201-2013/Heat%20Exchangers.pdf>
- [11] Borgnakke, C. and Sonntag, R. E., 2013, *Fundamentals of Thermodynamics Eighth Edition*, John Wiley and Sons, Hoboken, NJ.
- [12] 2018, “Water - Prandtl Number vs. Temperature and Pressure,” The Engineering Toolbox, accessed Apr. 3, 2024, https://www.engineeringtoolbox.com/water-steam-Prandtl-number-d_2059.html
- [13] Bergman, T. L., Lavine, A. S., Incropera, F. P., and Dewitt, D. P., 2016, *Fundamentals of Heat and Mass Transfer Seventh Edition*, John Wiley and Sons, Hoboken, NJ.
- [14] Ortiz, F. G., 2011, “Modeling of fire-tube boilers,” accessed Apr. 4, 2024, https://www.sciencedirect.com/science/article/pii/S1359431111003425?casa_token=dho50n0hDB8AAAAA:a6y5psv5Cr5oNwGNLFEFzyq3qzJJf1JFDQh564iipMGVFI3gdD-_63-fBg0Y16baex0IqfEOsg
- [15] Xin, T., Xu, C., and Yang, Y., 2020, “A general and simple method for evaluating the performance of the modified steam Rankine cycle: Thermal cycle splitting analytical method,” accessed Feb. 16, 2024, https://www.sciencedirect.com/science/article/pii/S0196890420302508?casa_token=NiD6G8hMMC8AAAAA:8XVSiX7uFuPAA5nfWt2Z7zJcZYjjsteq1jt9pgNj4WRIJzIKS5uenL04W-T8YfxUOyU7VeDJNg#0030
- [16] Elahifar, S., Assareh, E., and Nedaei, M., 2018, “Exergy analysis and optimization of the Rankine cycle in steam power plants using the firefly algorithm,” accessed Feb. 16, 2024, <https://www.mechanics-industry.org/articles/meca/full.html/2018/05/mi160223/mi160223.html#T2>
- [17] Dincer, I., 2018, “Comprehensive Energy Systems,” accessed Apr. 4, 2024, <https://www.sciencedirect.com/referencework/9780128149256/comprehensive-energy-systems>
- [18] Ferraro, V., Marinelli, V., Settino, J., and Nicoletti, F., 2020, “Techno-Economic Analysis of a Solar Tower Power Plant with an Open Air Brayton Cycle and a Combined Cycle - A Simplified Calculation Method,” accessed March 5, 2024, https://www.researchgate.net/profile/Francesco-Nicoletti/publication/346553201_Techno-Economic_Analysis_of_a_Solar_Tower_Power_Plant_with_an_Open_Air_Brayton_Cycle_and_a_Combined_Cycle_-_A_Simplified_Calculation_Method/links/60c344e4299bf1949f4a596a/

Appendix A: Rankine Cycle MATLAB Code

Below is the MATLAB for the Rankine Cycle efficiency calculations.

```
1  clc
2  clear all
3
4  % known variables
5  P23=10;
6  P14=.07384;
7  x4=.88;
8  T3U=400;
9  T1=40;
10 h1=XSteam('hL-T',T1);
11 nt=.9;
12 Qb=30*10^6;
13 S1=.5724;
14 D=25*10^-3;
15 L=10;
16 U=1000;
17 Tci=18.3;
18 Tco=21.1;
19 epsilon=.0015*10^-3;
20 Cp=4.18*10^3;
21 rho=999;
22 mu=1.12*10^-3;
23
24 %solving for lower bound of turbine inlet temp
25 s4f=XSteam('sL-p',P14);
26 s4g=XSteam('sV-p',P14);
27 s4=(1-x4)*s4f+x4*s4g;
28 T3L=XSteam('T-ps',P23,s4);
29
30 %initialize output array
31 temp=[];
32 eff=[];
33 var_min=T3L;
34 var_max=T3U;
35 step=.1;
36
37 for T3= var_min:step:var_max
38     %solving for the boiler
39     T2=XSteam('T-ps',P23,S1);
40     h2=XSteam('h-ps',P23,S1);
41     h3=XSteam('h-pT',P23, T3);
42     m_dot=Qb/(h3-h2);
43
44     % solving the turbine portion of the problem
45     S3=XSteam('s-pT',P23,T3);
46     h4s=XSteam('h-ps',P14,S3);
47     h4=nt*(h3-h4s)+h3;
48     Wt=m_dot*(h4-h3);
49
50     %solving for Rankine pump
51     Wp1=m_dot*(h2-h1);
52
```



```

53     %energy balance to find Qc
54     Qc=Qb+Wp1-Wt;
55
56     %solving for condenser
57     Δ_T1=abs(T1-Tci);
58     Δ_T2=abs(T1-Tco);
59     Δ_T=(Δ_T1-Δ_T2)/(log(Δ_T1/Δ_T2));
60     N=Qc/(U*Δ_T*pi*D*L);
61
62
63     %finding major loss and friction coefficient
64     m_dot_cooling_total=Qc/(Cp*(Tco-Tci));
65     m_dot_cooling=m_dot_cooling_total/N;
66     V=(m_dot_cooling)/(rho*pi*(D/2)^2);
67     Reynolds= (rho*V*D)/mu;
68     f=((1)/(-1.8*log10(((epsilon/D)/3.7)^1.11*(6.9/Reynolds))))^2;
69     Maj_loss=((f*L*rho*V^2)*N)/(2*D);
70
71     %cooling pump
72     flow_rate=V*pi*(D/2)^2;
73     Wp2=flow_rate*Maj_loss;
74
75     %overall rankine efficiency
76     nth= (Wt-Wp1-Wp2)/Qb;
77
78     %output array building
79     temp=[temp,T3];
80     eff=[eff,nth];
81 end
82
83 %efficiency plot
84 plot(temp,eff, "blue");
85 hold on
86 plot(T3,nth,"red*");
87 legend("Efficiency as a Function of Temperature","Maximum Efficiency")
88 xlabel("Turbine Inlet Temperature ( C )");
89 ylabel("Rankine Efficiency");
90 title("Rankine Cycle Efficiency as a Function of Turbine Inlet Temperature");
91 grid on;

```

Below is the excel sheet used for the Brayton cycle calculations.

33

100	70	17	674.0282	834.32665	534.1239	534.1238727	3.00E+04	8.78E+02	3.21E+05	4.70E+05	5.85E+05	3.60E+01	1.16E+05
100	70	18	685.1261	850.180209	525.4724	525.4723774	3.00E+04	1.17E+03	4.12E+05	6.48E+05	7.94E+05	3.55E+01	1.46E+05
100	70	19	695.792	865.417132	517.4178	517.4177728	3.00E+04	1.72E+03	5.76E+05	9.74E+05	1.18E+06	3.50E+01	2.02E+05
100	70	20	706.0641	880.091526	509.8906	509.8905655	3.00E+04	3.02E+03	9.70E+05	1.76E+06	2.09E+06	3.44E+01	3.34E+05
100	70	21	715.9756	894.250796	502.8323	502.8323304	3.00E+04	1.05E+04	3.24E+06	6.29E+06	7.38E+06	3.37E+01	1.09E+06
100	70	22	725.5554	907.936318	496.1935	496.1935175	3.00E+04	-7.85E+03	-2.30E+06	-4.79E+06	-5.55E+06	3.28E+01	-7.56E+05
100	70	23	734.8291	921.184439	489.9318	489.9317709	3.00E+04	-2.97E+03	-8.31E+05	-1.85E+06	-2.12E+06	3.19E+01	-2.65E+05
100	70	24	743.8191	934.02728	484.0106	484.0106238	3.00E+04	-1.97E+03	-4.99E+05	1.13E+06	1.34E+06	3.08E+01	1.54E+05
100	70	25	752.5454	946.49338	478.3985	478.3984739	3.00E+04	-1.38E+03	-3.52E+05	-8.98E+05	-1.00E+06	2.96E+01	-1.04E+05
100	70	26	761.0258	958.60822	473.0678	473.0677698	3.00E+04	-1.11E+03	-2.69E+05	-7.34E+05	-8.10E+05	2.83E+01	-7.61E+04
100	70	27	769.2763	970.394657	467.9944	467.9943593	3.00E+04	-9.34E+02	-2.15E+05	-6.28E+05	-6.86E+05	2.68E+01	-5.78E+04
100	70	28	777.3113	981.873277	463.157	463.1569619	3.00E+04	-8.11E+02	-1.78E+05	-5.55E+05	-6.00E+05	2.52E+01	-4.48E+04
100	70	29	785.1439	993.062697	458.5367	458.536739	3.00E+04	-7.21E+02	-1.50E+05	-5.01E+05	-5.36E+05	2.34E+01	-3.50E+04
100	70	30	792.7859	1003.97981	454.1169	454.1169408	3.00E+04	-6.51E+02	-1.28E+05	-4.60E+05	-4.88E+05	2.14E+01	-2.74E+04

Turbine Efficiency	Compressor Efficiency	Pressure Ratio	T2s	T2	T4s	T4	Q_L	Mdot	Q_h	W_c	W_t	Efficiency	W_net
90	100	5	475.1459	475.145883	757.6795	801.9115167	3.00E+04	9.90E+01	7.20E+04	1.74E+04	3.96E+04	3.08E+01	2.22E+04
90	100	6	500.5531	500.553132	719.2228	767.3005011	3.00E+04	1.12E+02	7.85E+04	2.25E+04	4.86E+04	3.32E+01	2.61E+04
90	100	7	523.0917	523.09171	688.235	739.4114732	3.00E+04	1.25E+02	8.49E+04	2.80E+04	5.77E+04	3.51E+01	2.98E+04
90	100	8	543.4342	543.434199	662.4734	716.2260488	3.00E+04	1.38E+02	9.11E+04	3.38E+04	6.71E+04	3.66E+01	3.33E+04
90	100	9	562.0332	562.033201	640.5517	696.4964041	3.00E+04	1.52E+02	9.74E+04	4.00E+04	7.69E+04	3.78E+01	3.69E+04
90	100	10	579.2093	579.209319	621.5574	679.4016661	3.00E+04	1.67E+02	1.04E+05	4.67E+04	8.71E+04	3.89E+01	4.04E+04
90	100	11	595.1988	595.198766	604.8607	664.3748152	3.00E+04	1.82E+02	1.10E+05	5.39E+04	9.78E+04	3.98E+01	4.39E+04
90	100	12	610.1811	610.181103	590.0097	651.0087451	3.00E+04	1.98E+02	1.17E+05	6.16E+04	1.09E+05	4.05E+01	4.74E+04
90	100	13	624.2963	624.296333	576.6704	639.0033245	3.00E+04	2.15E+02	1.24E+05	7.00E+04	1.21E+05	4.11E+01	5.11E+04
90	100	14	637.6559	637.655937	564.5891	628.130163	3.00E+04	2.32E+02	1.32E+05	7.91E+04	1.34E+05	4.16E+01	5.48E+04
90	100	15	650.3503	650.350276	553.5693	618.212343	3.00E+04	2.53E+02	1.39E+05	8.89E+04	1.48E+05	4.21E+01	5.87E+04
90	100	16	662.4537	662.453708	543.4557	609.1101512	3.00E+04	2.74E+02	1.48E+05	9.97E+04	1.62E+05	4.25E+01	6.28E+04
90	100	17	674.0282	674.028235	534.1239	600.7114854	3.00E+04	2.97E+02	1.57E+05	1.11E+05	1.79E+05	4.28E+01	6.71E+04
90	100	18	685.1261	685.126147	525.4724	592.9251397	3.00E+04	3.22E+02	1.66E+05	1.24E+05	1.96E+05	4.31E+01	7.17E+04
90	100	19	695.792	695.791993	517.4178	585.6799955	3.00E+04	3.49E+02	1.77E+05	1.39E+05	2.15E+05	4.33E+01	7.65E+04
90	100	20	706.0641	706.064068	509.8906	579.9015089	3.00E+04	3.79E+02	1.89E+05	1.54E+05	2.39E+05	4.35E+01	8.19E+04
90	100	21	715.9756	715.975557	502.8323	572.5490973	3.00E+04	4.12E+02	2.00E+05	1.72E+05	2.59E+05	4.37E+01	8.74E+04
90	100	22	725.5554	725.555422	496.1935	566.5741657	3.00E+04	4.49E+02	2.14E+05	1.92E+05	2.85E+05	4.38E+01	9.37E+04
90	100	23	734.8291	734.829107	489.9318	560.9385938	3.00E+04	4.90E+02	2.29E+05	2.14E+05	3.15E+05	4.39E+01	1.01E+05
90	100	24	743.8191	743.819096	484.0106	555.6095614	3.00E+04	5.37E+02	2.46E+05	2.39E+05	3.48E+05	4.40E+01	1.08E+05
90	100	25	752.5454	752.545366	478.3985	550.5586265	3.00E+04	5.91E+02	2.66E+05	2.69E+05	3.85E+05	4.40E+01	1.17E+05
90	100	26	761.0258	761.025754	473.0678	545.7609929	3.00E+04	6.53E+02	2.88E+05	3.02E+05	4.29E+05	4.40E+01	1.27E+05
90	100	27	769.2763	769.27626	467.9944	541.1394024	3.00E+04	7.25E+02	3.14E+05	3.42E+05	4.80E+05	4.40E+01	1.38E+05
90	100	28	777.3113	777.311294	463.157	539.8412657	3.00E+04	8.11E+02	3.44E+05	3.89E+05	5.40E+05	4.40E+01	1.51E+05
90	100	29	785.1439	785.143888	458.5367	532.6830651	3.00E+04	9.14E+02	3.81E+05	4.45E+05	6.13E+05	4.39E+01	1.67E+05
90	100	30	792.7859	792.785866	454.1169	528.7052468	3.00E+04	1.04E+03	4.26E+05	5.15E+05	7.02E+05	4.38E+01	1.87E+05

Turbine Efficiency	Compressor Efficiency	Pressure Ratio	T2s	T2	T4s	T4	Q_L	Mdot	Q_h	W_c	W_t	Efficiency	W_net
80	100	5	475.1459	475.145883	757.6795	846.1435704	3.00E+04	8.63E+01	6.28E+04	1.52E+04	3.07E+04	2.47E+01	1.55E+04
80	100	6	500.5531	500.553132	719.2228	815.3782232	3.00E+04	9.47E+01	6.65E+04	1.91E+04	3.66E+04	2.63E+01	1.75E+04
80	100	7	523.0917	523.09171	688.235	790.5879762	3.00E+04	1.03E+02	6.99E+04	2.30E+04	4.23E+04	2.75E+01	1.92E+04
80	100	8	543.4342	543.434199	662.4734	769.97871	3.00E+04	1.11E+02	7.30E+04	2.71E+04	4.78E+04	2.84E+01	2.07E+04
80	100	9	562.0332	562.033201	640.5517	752.441381	3.00E+04	1.19E+02	7.59E+04	3.11E+04	5.32E+04	2.91E+01	2.29E+04
80	100	10	579.2093	579.209319	621.5574	737.2490254	3.00E+04	1.28E+02	7.85E+04	3.53E+04	5.85E+04	2.96E+01	2.32E+04
80	100	11	595.1988	595.198766	604.8607	723.8885468	3.00E+04	1.33E+02	8.10E+04	3.96E+04	6.38E+04	2.99E+01	2.42E+04
80	100	12	610.1811	610.181103	590.0097	712.0077734	3.00E+04	1.41E+02	8.35E+04	4.39E+04	6.91E+04	3.01E+01	2.52E+04
80	100	13	624.2963	624.296333	576.6704	701.3362884	3.00E+04	1.48E+02	8.58E+04	4.83E+04	7.43E+04	3.03E+01	2.60E+04
80	100	14	637.6559	637.655937	564.5891	691.671256	3.00E+04	1.56E+02	8.80E+04	5.28E+04	7.96E+04	3.04E+01	2.67E+04
80	100	15	650.3503	650.350276	553.5693	682.855416	3.00E+04	1.65E+02	9.02E+04	5.75E+04	8.48E+04	3.03E+01	2.74E+04
80	100	16	662.4537	662.453708	543.4557	674.7645788	3.00E+04	1.71E+02	9.23E+04	6.22E+04	9.02E+04	3.03E+01	2.79E+04
80	100	17	674.0282	674.028235	534.1239	667.2900981	3.00E+04	1.79E+02	9.43E+04	6.71E+04	9.55E+04	3.02E+01	2.85E+04
80	100	18	685.1261	685.126147	525.4724	660.3779019	3.00E+04	1.86E+02	9.63E+04	7.20E+04	1.01E+05	3.00E+01	2.89E+04
80	100	19	695.792	695.791993	517.4178	653.9342183	3.00E+04	1.94E+02	9.83E+04	7.71E+04	1.06E+05	2.98E+01	2.93E+04
80	100	20	706.0641	706.064068	509.8906	647.9124524	3.00E+04	2.02E+02	1.00E+05	8.24E+04	1.12E+05	2.96E+01	2.96E+04
80	100	21	715.9756	715.975557	502.8323	642.2658843	3.00E+04	2.10E+02	1.02E+05	8.77E+04	1.19E+05	2.93E+01	2.99E+04
80	100	22	725.5554	725.555422	496.1935	636.954414	3.00E+04	2.18E+02	1.04E+05	9.32E+04	1.22E+05	2.90E+01	3.01E+04
80	100	23	734.8291	734.829107	489.9318	631.9454167	3.00E+04	2.28E+02	1.06E+05	9.89E+04	1.29E+05	2.86E+01	3.03E+04
80	100	24	743.8191	743.819096	484.0106	627.208499	3.00E+04	2.35E+02	1.08E+05	1.05E+05	1.35E+05	2.83E+01	3.04E+04
80	100	25	752.5454	752.545366	478.3985	622.7187791	3.00E+04	2.43E+02	1.09E+05	1.11E+05	1.41E+05	2.79E+01	3.05E+04
80	100	26	761.0258	761.025754	473.0678	618.4542159	3.00E+04	2.52E+02	1.11E+05	1.17E+05	1.47E+05	2.75E+01	3.05E+04
80	100	27	769.2763	769.27626	467.9944	614.3954875	3.00E+04	2.61E+02	1.13E+05	1.23E+05	1.54E+05	2.70E+01	3.05E+04
80	100	28	777.3113	777.311294	463.157	610.5255955	3.00E+04	2.70E+02	1.15E+05	1.30E+05	1.60E+05	2.65E+01	3.04E+04
80	100	29	785.1439	785.143888	458.5367	606.8293912	3.00E+04	2.80E+02	1.17E+05	1.36E+05	1.67E+05	2.60E+01	3.03E+04
80	100	30	792.7859	792.785866	454.1169	603.2935527	3.00E+04	2.89E+02	1.18E+05	1.43E+05	1.73E+05	2.55E+01	3.02E+04

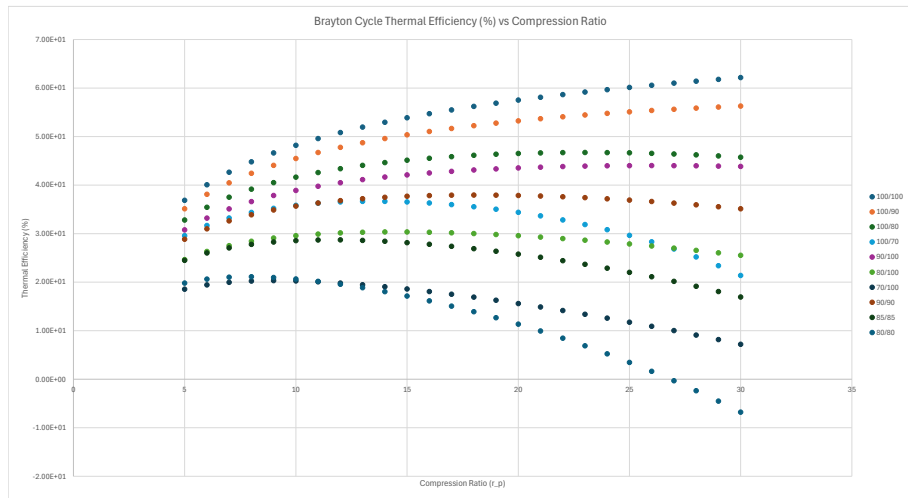
Turbine Efficiency	Compressor Efficiency	Pressure Ratio	T2s	T2	T4s	T4	Q_L	Mdot	Q_h	W_c	W_t	Efficiency	W_net
70	100	5	475.1459	475.145883	757.6795	890.3756241	3.00E+04	7.65E+01	5.57E+04	1.35E+04	2.38E+04	1.86E+01	1.03E+04
70	100	6	500.5531	500.553132	719.2228	863.4559453	3.00E+04	8.22E+01	5.77E+04	1.66E+04	2.78E+04	1.94E+01	1.12E+04
70	100	7	523.0917	523.09171	688.235	841.7644792	3.00E+04	8.74E+01	5.94E+04	1.96E+04	3.14E+04	2.00E+01	1.19E

90	90	5	475.1459	494.606536	757.6795	801.9115167	3.00E+04	9.90E+01	7.01E+04	1.93E+04	3.96E+04	2.88E+01	2.02E+04
90	90	6	500.5531	522.836814	719.2228	767.3005011	3.00E+04	1.12E+02	7.60E+04	2.50E+04	4.86E+04	3.10E+01	2.36E+04
90	90	7	523.0917	547.879678	688.235	739.4114732	3.00E+04	1.25E+02	8.17E+04	3.11E+04	5.77E+04	3.26E+01	2.67E+04
90	90	8	543.4342	570.482443	662.4734	716.2260488	3.00E+04	1.38E+02	8.73E+04	3.75E+04	6.71E+04	3.39E+01	2.96E+04
90	90	9	562.0332	591.148002	640.5517	696.4964941	3.00E+04	1.52E+02	9.30E+04	4.45E+04	7.69E+04	3.49E+01	3.24E+04
90	90	10	579.2093	610.232576	621.5574	679.4016661	3.00E+04	1.67E+02	9.86E+04	5.19E+04	8.71E+04	3.57E+01	3.52E+04
90	90	11	595.1988	627.996629	604.8607	664.3746152	3.00E+04	1.82E+02	1.04E+05	5.99E+04	9.78E+04	3.63E+01	3.79E+04
90	90	12	610.1811	644.54567	590.0097	651.0087451	3.00E+04	1.98E+02	1.10E+05	6.85E+04	1.09E+05	3.68E+01	4.06E+04
90	90	13	624.2963	660.329259	576.6704	639.0033245	3.00E+04	2.15E+02	1.16E+05	7.78E+04	1.21E+05	3.72E+01	4.32E+04
90	90	14	637.6559	675.173264	564.5891	628.130103	3.00E+04	2.33E+02	1.23E+05	8.78E+04	1.34E+05	3.75E+01	4.61E+04
90	90	15	650.3503	689.278084	553.5693	618.212343	3.00E+04	2.53E+02	1.30E+05	9.88E+04	1.48E+05	3.77E+01	4.89E+04
90	90	16	662.4537	702.726342	543.4557	609.1101512	3.00E+04	2.74E+02	1.37E+05	1.11E+05	1.62E+05	3.78E+01	5.17E+04
90	90	17	674.0282	715.596928	534.1239	600.7114854	3.00E+04	2.97E+02	1.44E+05	1.24E+05	1.79E+05	3.79E+01	5.47E+04
90	90	18	685.1261	727.917941	525.4724	592.9251397	3.00E+04	3.22E+02	1.52E+05	1.38E+05	1.96E+05	3.80E+01	5.79E+04
90	90	19	695.792	739.768881	517.4178	585.6759955	3.00E+04	3.49E+02	1.61E+05	1.54E+05	2.15E+05	3.79E+01	6.11E+04
90	90	20	706.0641	751.182298	509.8906	578.9015089	3.00E+04	3.79E+02	1.71E+05	1.72E+05	2.36E+05	3.79E+01	6.46E+04
90	90	21	715.9756	762.195063	502.8323	572.5490973	3.00E+04	4.12E+02	1.81E+05	1.91E+05	2.59E+05	3.77E+01	6.83E+04
90	90	22	725.5554	772.839358	496.1935	566.5741657	3.00E+04	4.49E+02	1.92E+05	2.13E+05	2.85E+05	3.76E+01	7.24E+04
90	90	23	734.8291	783.143452	489.9318	560.9385938	3.00E+04	4.90E+02	2.05E+05	2.38E+05	3.15E+05	3.74E+01	7.68E+04
90	90	24	743.8191	793.133229	484.0106	555.6995614	3.00E+04	5.37E+02	2.19E+05	2.66E+05	3.46E+05	3.72E+01	8.16E+04
90	90	25	752.5454	802.828184	478.2985	550.5586265	3.00E+04	5.91E+02	2.36E+05	2.98E+05	3.85E+05	3.69E+01	8.70E+04
90	90	26	761.0258	812.250838	473.0678	545.7609929	3.00E+04	6.53E+02	2.54E+05	3.36E+05	4.29E+05	3.66E+01	9.31E+04
90	90	27	769.2763	821.418067	467.9944	541.1949234	3.00E+04	7.25E+02	2.76E+05	3.80E+05	4.80E+05	3.63E+01	1.00E+05
90	90	28	777.3113	830.345882	463.157	536.8412657	3.00E+04	8.11E+02	3.01E+05	4.32E+05	5.40E+05	3.59E+01	1.08E+05
90	90	29	785.1439	839.048764	458.5367	532.6830651	3.00E+04	9.14E+02	3.31E+05	4.95E+05	6.13E+05	3.55E+01	1.18E+05
90	90	30	792.7859	847.539851	454.1169	528.7052468	3.00E+04	1.04E+03	3.68E+05	5.72E+05	7.02E+05	3.51E+01	1.29E+05

Turbine Efficiency	Compressor Efficiency	Pressure Ratio	T2s	T2	T4s	T4	Q_L	Mdot	Q_h	W_c	W_t	Efficiency	W_net
85	85	5	475.1459	506.05398	757.6795	824.0275436	3.00E+04	9.22E+01	6.42E+04	1.91E+04	3.48E+04	2.45E+01	1.57E+04
85	85	6	500.5531	535.944862	719.2228	791.3393922	3.00E+04	1.03E+02	6.84E+04	2.43E+04	4.21E+04	2.60E+01	1.78E+04
85	85	7	523.0917	562.460836	688.235	764.9897247	3.00E+04	1.13E+02	7.22E+04	2.97E+04	4.92E+04	2.71E+01	1.95E+04
85	85	8	543.4342	586.393175	662.4734	743.1023794	3.00E+04	1.23E+02	7.57E+04	3.53E+04	5.84E+04	2.78E+01	2.10E+04
85	85	9	562.0332	608.274355	640.5517	724.4689111	3.00E+04	1.33E+02	7.91E+04	4.12E+04	6.36E+04	2.83E+01	2.24E+04
85	85	10	579.2093	628.481551	621.5574	708.3237957	3.00E+04	1.43E+02	8.23E+04	4.73E+04	7.08E+04	2.86E+01	2.35E+04
85	85	11	595.1988	647.292666	604.8607	694.131581	3.00E+04	1.54E+02	8.54E+04	5.37E+04	7.82E+04	2.87E+01	2.45E+04
85	85	12	610.1811	664.918945	590.0097	681.5082593	3.00E+04	1.65E+02	8.84E+04	6.03E+04	8.57E+04	2.87E+01	2.54E+04
85	85	13	624.2963	681.525098	576.6704	670.1698965	3.00E+04	1.76E+02	9.14E+04	6.73E+04	9.34E+04	2.86E+01	2.61E+04
85	85	14	637.6559	697.242279	564.5891	659.9007905	3.00E+04	1.87E+02	9.43E+04	7.45E+04	1.01E+05	2.84E+01	2.68E+04
85	85	15	650.3503	712.176795	553.5693	650.5337995	3.00E+04	1.98E+02	9.72E+04	8.21E+04	1.10E+05	2.81E+01	2.74E+04
85	85	16	662.4537	726.416127	543.4557	641.937365	3.00E+04	2.11E+02	1.00E+05	9.01E+04	1.18E+05	2.78E+01	2.78E+04
85	85	17	674.0282	740.033217	534.1239	634.0052918	3.00E+04	2.23E+02	1.03E+05	9.85E+04	1.27E+05	2.74E+01	2.82E+04
85	85	18	685.1261	753.089584	525.4724	626.6515208	3.00E+04	2.36E+02	1.06E+05	1.07E+05	1.36E+05	2.69E+01	2.85E+04
85	85	19	695.792	765.637638	517.4178	618.8051069	3.00E+04	2.49E+02	1.09E+05	1.17E+05	1.45E+05	2.64E+01	2.87E+04
85	85	20	706.0641	777.722453	509.8906	613.4698907	3.00E+04	2.63E+02	1.12E+05	1.26E+05	1.55E+05	2.58E+01	2.88E+04
85	85	21	715.9756	789.383008	502.8323	607.4074808	3.00E+04	2.78E+02	1.15E+05	1.37E+05	1.68E+05	2.51E+01	2.88E+04
85	85	22	725.5554	800.653438	496.1935	601.7644899	3.00E+04	2.94E+02	1.18E+05	1.48E+05	1.76E+05	2.44E+01	2.88E+04
85	85	23	734.8291	811.563655	489.9318	596.4420052	3.00E+04	3.10E+02	1.21E+05	1.59E+05	1.88E+05	2.37E+01	2.87E+04
85	85	24	743.8191	822.140113	484.0106	591.4090302	3.00E+04	3.27E+02	1.24E+05	1.71E+05	2.00E+05	2.29E+01	2.84E+04
85	85	25	752.5454	832.406313	478.2985	586.6387028	3.00E+04	3.45E+02	1.27E+05	1.84E+05	2.12E+05	2.20E+01	2.80E+04
85	85	26	761.0258	842.38324	473.0678	582.1076944	3.00E+04	3.64E+02	1.31E+05	1.98E+05	2.26E+05	2.11E+01	2.76E+04
85	85	27	769.2763	852.089718	467.9944	577.7952054	3.00E+04	3.84E+02	1.34E+05	2.13E+05	2.40E+05	2.02E+01	2.70E+04
85	85	28	777.3113	861.542699	463.157	573.6834176	3.00E+04	4.06E+02	1.38E+05	2.29E+05	2.55E+05	1.91E+01	2.64E+04
85	85	29	785.1439	870.757515	458.5367	569.7662281	3.00E+04	4.28E+02	1.42E+05	2.45E+05	2.71E+05	1.81E+01	2.56E+04
85	85	30	792.7859	879.748078	454.1169	565.9993997	3.00E+04	4.53E+02	1.46E+05	2.64E+05	2.88E+05	1.69E+01	2.47E+04

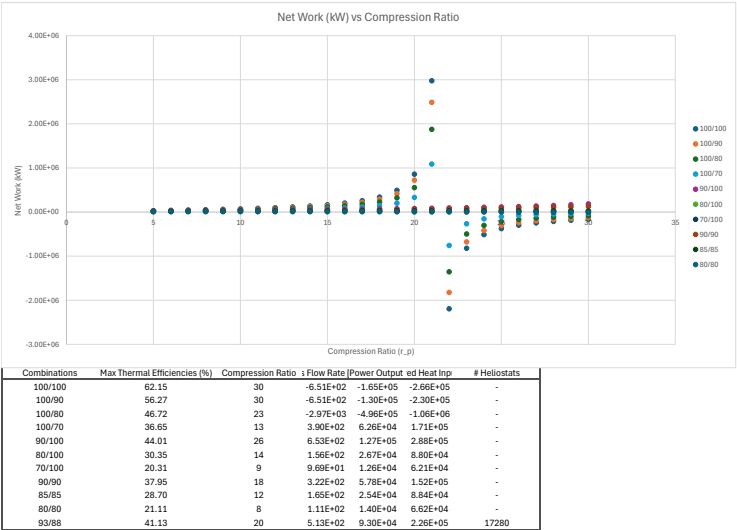
Turbine Efficiency	Compressor Efficiency	Pressure Ratio	T2s	T2	T4s	T4	Q_L	Mdot	Q_h	W_c	W_t	Efficiency	W_net
80	80	5	475.1459	518.932353	757.6795	846.1435704	3.00E+04	8.63E+01	5.90E+04	1.90E+04	3.07E+04	1.98E+01	1.17E+04
80	80	6	500.5531	550.691415	719.2228	815.3782232	3.00E+04	9.47E+01	6.18E+04	2.38E+04	3.66E+04	2.06E+01	1.27E+04
80	80	7	523.0917	578.854638	688.235	790.5879762	3.00E+04	1.03E+02	6.41E+04	2.88E+04	4.23E+04	2.10E+01	1.35E+04
80	80	8	543.4342	604.292748	662.4734	769.97971	3.00E+04	1.11E+02	6.62E+04	3.38E+04	4.79E+04	2.11E+01	1.40E+04
80	80	9	562.0332	627.541502	640.5517	752.4413281	3.00E+04	1.18E+02	6.80E+04	3.89E+04	5.32E+04	2.10E+01	1.43E+04
80	80	10	579.2093	649.011648	621.5574	737.2459254	3.00E+04	1.26E+02	6.97E+04	4.41E+04	5.85E+04	2.06E+01	1.44E+04
80	80	11	595.1988	668.998457	604.8607	723.8885468	3.00E+04	1.33E+02	7.12E+04	4.94E+04	6.38E+04	2.02E+01	1.44E+04
80	80	12	610.1811	687.726379	590.0097	712.0077734	3.00E+04	1.41E+02	7.25E+04	5.49E+04	6.91E+04	1.96E+01	1.42E+04
80	80	13	624.2963	705.370416	576.6704	701.3362884	3.00E+04	1.48E+02	7.37E+04	6.04E+04	7.43E+04	1.89E+01	1.39E+04
80	80	14	637.6559	722.069922	564.5891	691.671256	3.00E+04	1.56E+02	7.48E+04	6.61E+04	7.96E+04	1.80E+01	1.35E+04
80	80	15	650.3503	737.937845	553.5693	682.855416	3.00E+04	1.63E+02	7.58E+04	7.18E+04	8.48E+04	1.71E+01	1.30E+04
80	80	16	662.4537	753.067135	543.4557	674.7645788	3.00E+04	1.71E+02	7.67E+04	7.78E+04	9.02E+04	1.61E+01	1.24E+04
80	80	17	674.0282	767.535294	534.1239	667.2990981	3.00E+04	1.79E+02	7.75E+04	8.38E+04	9.55E+04	1.51E+01	1.17E+04
80	80	18	685.1261	781.407683	525.4724	660.3779019	3.00E+04	1.86E+02	7.83E+04	9.01E+04	1.01E+05	1.39E+01	1.09E+04
80	80	19	695.792	794.739991	517.4178	653.9342183	3.00E+04	1.94E+02	7.90E+04	9.64E+04	1.06E+05	1.27E+01	1.00E+04
80	80	20	706.0641	807.580085	509.8906	647.9124524	3.00E+04	2.02E+02	7.98E+04	1.03E+05	1.12E+05	1.13E+01	9.03E+03
80	80	21	715.9756	819.969446	502.8323	642.2636843	3.00E+04	2.10E+02	8.01E+04	1.10E+05	1.18E+05	9.94E+00	7.96E+03
80	80	22	725.5554	831.944278	496.1935	636.954814	3.00E+04	2.18E+02	8.06E+04	1.17E+05	1.23E+05	8.95E+00	6.81E+03
80	80	23	734.8291	843.526384	489.0318	631.0276019	3.00E+04	2.26E+02	8.13E+04	1.24E+05	1.29E+05	8.07E+00	5.67E+03
80	80	24	743.8191	854.77387	484.0106	627.208499	3.00E+04	2.35E+02	8.14E+04	1.31E+05	1.35E+05	7.25E+00	4.25E+03
80	80	25	752.5454	865.681707	478.3985	623.787091	3.00E+04	2.43E+02	8.17E+04	1.38E+05	1.41E+05	6.47E+00	2.84E+03
80	80	26	761.0258	876.28193	473.0678	618.454219	3.00E+04	2.52E+02	8.20E+04	1.46E+05	1.47E+05	5.63E+00	1.63E+03
80	80	27	769.2763	886.595325	467.9044	614.3954785	3.00E+04	2.61E+02	8.22E+04	1.54E+05	1.54E+05	-3.16E+01	-2.30E+02
80	80	28	777.3115	896.63918	463.157	610.5256959	3.00E+04	2.70E+02	8.25E+04	1.62E+05	1.62E+05	-1.94E+02	-1.94E+02
80	80	29	785.1439	906.42986	458.5367	606.9203912	3.00E+04	2.80E+02	8.24E+04	1.70E+05	1.67E+05	-4.52E+02	-3.72E+02
80	80	30	792.7859	915.982333	454.1169	603.293527	3.00E+04	2.89E+02	8.25E+04	1.79E+05	1.73E+05	-6.79E+02	-5.60E+03

Pressure Ratio	100/100	100/90	100/80	100/70	90/100	80/100	70/100	90/90	85/85	80/80
5	3.89E+01	3.51E+01	3.28E+01	2.96E+01	3.08E+01		2.47E+01	1.88E+01	2.88E+01	2.45E+01
6	4.01E+01	3.81E+01	3.54E+01	3.17E+01	3.32E+01		2.53E+01	1.94E+01	3.10E+01	2.60E+01
7	4.26E+01	4.05E+01	3.75E+01	3.32E+01	3.51E+01		2.75E+01	2.00E+01	3.26E+01	2.71E+01
8	4.48E+01	4.24E+01	3.92E+01	3.44E+01	3.66E+01		2.84E+01	2.02E+01	3.39E+01	2.78E+01
9	4.66E+01	4.41E+01	4.05E+01	3.52E+01	3.78E+01		2.91E+01	2.03E+01	3.49E+01	2.83E+01
10	4.82E+01	4.55E+01	4.18E+01	3.58E+01	3.89E+01		2.96E+01	2.02E+01	3.57E+01	2.86E+01
11	4.96E+01	4.67E+01	4.26E+01	3.63E+01	3.98E+01		2.99E+01	2.01E+01	3.63E+01	2.87E+01
12	5.08E+01	4.78E+01	4.34E+01	3.65E+01	4.05E+01		3.01E+01	1.99E+01	3.68E+01	2.87E+01
13	5.19E+01	4.87E+01	4.41E+01	3.66E+01	4.11E+01		3.03E+01	1.95E+01	3.72E+01	2.86E+01
14	5.29E+01	4.96E+01	4.46E+01	3.66E+01	4.16E+01		3.04E+01	1.91E+01	3.75E+01	2.84E+01
15	5.39E+01	5.04E+01	4.51E+01	3.65E+01	4.21E+01		3.03E+01	1.86E+01	3.77E+01	2.81E+01
16	5.47E+01	5.10E+01	4.55E+01	3.63E+01	4.25E+01		3.03E+01	1.81E+01	3.78E+01	2.78E+01
17	5.55E+01	5.17E+01	4.59E+01	3.60E+01	4.28E+01		3.02E+01	1.75E+01	3.79E+01	2.74E+01
18	5.62E+01	5.22E+01	4.61E+01	3.55E+01	4.31E+01		3.00E+01	1.69E+01	3.80E+01	2.69E+01
19	5.69E+01	5.28E+01	4.64E+01	3.50E+01	4.33E+01		2.98E+01	1.63E+01	3.79E+01	2.64E+01
20	5.75E+01	5.32E+01	4.65E+01	3.44E+01	4.35E+01		2.96E+01	1.56E+01	3.79E+01	2.58E+01
21	5.81E+01	5.37E+01	4.66E+01	3.37E+01	4.37E+01		2.93E+01	1.49E+01	3.77E+01	2.51E+01
22	5.86E+01	5.41E+01	4.67E+01	3.28E+01	4.38E+01		2.90E+01	1.41E+01	3.76E+01	2.44E+01
23	5.92E+01	5.44E+01	4.67E+01	3.19E+01	4.39E+01		2.86E+01	1.34E+01	3.74E+01	2.37E+01
24	5.97E+01	5.48E+01	4.67E+01	3.08E+01	4.40E+01		2.83E+01	1.26E+01	3.72E+01	2.29E+01
25	6.01E+01	5.51E+01	4.66E+01	2.96E+01	4.40E+01		2.79E+01	1.17E+01	3.69E+01	2.20E+01
26	6.06E+01	5.54E+01	4.65E+01	2.83E+01	4.40E+01		2.75E+01	1.09E+01	3.66E+01	2.11E+01
27	6.10E+01	5.56E+01	4.64E+01	2.68E+01	4.40E+01		2.70E+01	1.00E+01	3.63E+01	2.02E+01
28	6.14E+01	5.59E+01	4.62E+01	2.52E+01	4.40E+01		2.65E+01	9.10E+00	3.59E+01	1.91E+01
29	6.18E+01	5.61E+01	4.60E+01	2.34E+01	4.39E+01		2.60E+01	8.17E+00	3.55E+01	1.81E+01
30	6.22E+01	5.63E+01	4.57E+01	2.14E+01	4.38E+01		2.55E+01	7.20E+00	3.51E+01	1.69E+01



Pressure Ratio	100/100	100/90	100/80	100/70	90/100	80/100	70/100	90/90	85/85	80/80
5	3.11E+04	2.88E+04	2.60E+04	2.24E+04	2.22E+04		1.55E+04	1.03E+04	2.02E+04	1.57E+04
6	3.83E+04	3.53E+04	3.15E+04	2.66E+04	2.61E+04		1.75E+04	1.12E+04	2.36E+04	1.78E+04
7	4.60E+04	4.21E+04	3.71E+04	3.08E+04	2.98E+04		1.92E+04	1.19E+04	2.67E+04	1.95E+04
8	5.43E+04	4.93E+04	4.31E+04	3.50E+04	3.33E+04		2.07E+04	1.23E+04	2.96E+04	2.10E+04
9	6.35E+04	5.73E+04	4.95E+04	3.95E+04	3.69E+04		2.20E+04	1.26E+04	3.24E+04	2.24E+04
10	7.38E+04	6.62E+04	5.66E+04	4.43E+04	4.04E+04		2.32E+04	1.28E+04	3.52E+04	2.35E+04
11	8.58E+04	7.64E+04	6.47E+04	4.96E+04	4.39E+04		2.42E+04	1.29E+04	3.79E+04	2.45E+04
12	9.99E+04	8.84E+04	7.41E+04	5.56E+04	4.74E+04		2.52E+04	1.28E+04	4.06E+04	2.54E+04
13	1.17E+05	1.03E+05	8.53E+04	6.26E+04	5.11E+04		2.60E+04	1.27E+04	4.33E+04	2.61E+04
14	1.38E+05	1.21E+05	9.91E+04	7.11E+04	5.48E+04		2.67E+04	1.26E+04	4.61E+04	2.68E+04
15	1.66E+05	1.44E+05	1.17E+05	8.17E+04	5.87E+04		2.74E+04	1.24E+04	4.89E+04	2.74E+04
16	2.03E+05	1.75E+05	1.40E+05	9.58E+04	6.28E+04		2.79E+04	1.21E+04	5.17E+04	2.78E+04
17	2.57E+05	2.20E+05	1.74E+05	1.16E+05	6.71E+04		2.85E+04	1.18E+04	5.47E+04	2.82E+04
18	3.41E+05	2.90E+05	2.27E+05	1.46E+05	7.17E+04		2.89E+04	1.15E+04	5.78E+04	2.85E+04
19	4.94E+05	4.18E+05	3.24E+05	2.02E+05	7.65E+04		2.93E+04	1.11E+04	6.11E+04	2.87E+04
20	8.62E+05	7.25E+05	5.54E+05	3.34E+05	8.18E+04		2.96E+04	1.07E+04	6.46E+04	2.88E+04
21	2.98E+06	2.49E+06	1.88E+06	1.09E+06	8.74E+04		2.99E+04	1.02E+04	6.83E+04	2.88E+04
22	-2.18E+06	-1.82E+06	-1.35E+06	-7.56E+05	9.37E+04		3.01E+04	9.71E+03	7.24E+04	2.89E+04
23	-8.20E+05	-6.76E+05	-4.96E+05	-2.65E+05	1.01E+05		3.03E+04	9.20E+03	7.68E+04	2.89E+04
24	-5.11E+05	-4.18E+05	-3.02E+05	-1.54E+05	1.08E+05		3.04E+04	8.66E+03	8.16E+04	2.84E+04
25	-3.74E+05	-3.04E+05	-2.17E+05	-1.04E+05	1.17E+05		3.05E+04	8.09E+03	8.70E+04	2.80E+04
26	-2.96E+05	-2.39E+05	-1.68E+05	-7.61E+04	1.27E+05		3.05E+04	7.51E+03	9.31E+04	2.76E+04

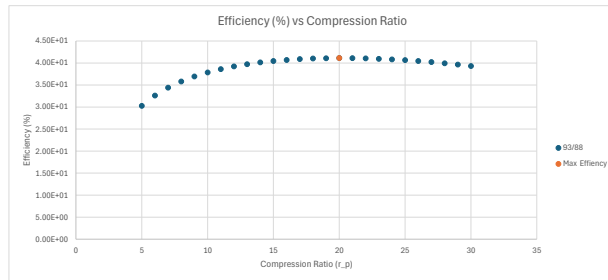
27	-2.46E+05	-1.97E+05	-1.39E+05	-5.78E+04	1.38E+05	3.05E+04	6.90E+03	1.00E+05	2.70E+04	-2.60E+02
28	-2.11E+05	-1.68E+05	-1.14E+05	-4.48E+04	1.51E+05	3.04E+04	6.27E+03	1.08E+05	2.64E+04	-1.94E+03
29	-1.85E+05	-1.46E+05	-9.77E+04	-3.50E+04	1.67E+05	3.03E+04	5.62E+03	1.18E+05	2.56E+04	-3.72E+03
30	-1.65E+05	-1.30E+05	-8.49E+04	-2.74E+04	1.87E+05	3.02E+04	4.95E+03	1.29E+05	2.47E+04	-5.60E+03



T1	T2	T3	T4	T5	P1=P4=P5	P2=P3							
	300		1200	500	100000								
Turbine Efficiency	Compressor Efficiency	Pressure Ratio	T2s	T2	T4s	T4	Q_L	Mdot	Q_h	W_c	W_t	Efficiency	W_net
93	88	5	475.1458826	499.0294	757.67946	788.6419006	3.00E+04	1.04E+02	7.29E+04	2.07E+04	4.28E+04	3.03E+01	2.21E+04
93	88	6	500.5531323	527.9013	719.22278	752.8771845	3.00E+04	1.18E+02	7.97E+04	2.70E+04	5.30E+04	3.26E+01	2.60E+04
93	88	7	523.0917103	553.5133	688.23497	724.0585224	3.00E+04	1.33E+02	8.66E+04	3.39E+04	6.37E+04	3.44E+01	2.98E+04
93	88	8	543.4341986	576.6298	662.47339	700.1002504	3.00E+04	1.49E+02	9.35E+04	4.15E+04	7.49E+04	3.58E+01	3.35E+04
93	88	9	562.0332014	597.765	640.55166	679.7130439	3.00E+04	1.66E+02	1.01E+05	4.97E+04	8.69E+04	3.69E+01	3.71E+04
93	88	10	579.2093187	617.2833	621.55741	662.0483863	3.00E+04	1.84E+02	1.08E+05	5.87E+04	9.96E+04	3.79E+01	4.09E+04
93	88	11	595.1987657	635.4531	604.86068	646.5204357	3.00E+04	2.04E+02	1.16E+05	6.87E+04	1.13E+05	3.86E+01	4.46E+04
93	88	12	610.1811029	652.4785	590.00972	632.7090366	3.00E+04	2.25E+02	1.24E+05	7.97E+04	1.28E+05	3.92E+01	4.86E+04
93	88	13	624.296333	668.5186	576.67036	620.3034353	3.00E+04	2.48E+02	1.33E+05	9.19E+04	1.45E+05	3.97E+01	5.27E+04
93	88	14	637.6559372	683.6999	564.58907	609.0678351	3.00E+04	2.74E+02	1.42E+05	1.06E+05	1.63E+05	4.01E+01	5.70E+04
93	88	15	650.3502758	698.1253	553.56927	598.8194211	3.00E+04	3.02E+02	1.52E+05	1.21E+05	1.83E+05	4.05E+01	6.16E+04
93	88	16	662.4537082	711.8792	543.45572	589.4138229	3.00E+04	3.34E+02	1.64E+05	1.38E+05	2.05E+05	4.07E+01	6.67E+04
93	88	17	674.0282349	725.0321	534.12387	580.7352016	3.00E+04	3.70E+02	1.76E+05	1.58E+05	2.30E+05	4.09E+01	7.22E+04
93	88	18	685.1261466	737.6433	525.47238	572.689311	3.00E+04	4.11E+02	1.91E+05	1.81E+05	2.59E+05	4.10E+01	7.83E+04
93	88	19	695.7919926	749.7636	517.41777	565.1985287	3.00E+04	4.58E+02	2.07E+05	2.07E+05	2.92E+05	4.11E+01	8.51E+04
93	88	20	706.0640681	761.4364	509.89057	558.1982259	3.00E+04	5.13E+02	2.26E+05	2.36E+05	3.31E+05	4.11E+01	9.30E+04
93	88	21	715.9755571	772.6995	502.83233	551.6340673	3.00E+04	5.79E+02	2.48E+05	2.75E+05	3.77E+05	4.11E+01	1.02E+05
93	88	22	725.5554223	783.5857	496.19352	545.4599713	3.00E+04	6.57E+02	2.75E+05	3.19E+05	4.32E+05	4.11E+01	1.13E+05
93	88	23	734.8291072	794.124	489.93177	539.6365469	3.00E+04	7.54E+02	3.07E+05	3.74E+05	5.00E+05	4.10E+01	1.26E+05
93	88	24	743.819096	804.3399	484.01062	534.1298801	3.00E+04	8.75E+02	3.48E+05	4.43E+05	5.85E+05	4.08E+01	1.42E+05
93	88	25	752.5453659	814.2561	478.39847	528.9105807	3.00E+04	1.03E+03	4.00E+05	5.34E+05	6.96E+05	4.07E+01	1.63E+05
93	88	26	761.0257542	823.8929	473.06777	523.953026	3.00E+04	1.25E+03	4.71E+05	6.56E+05	8.47E+05	4.05E+01	1.91E+05
93	88	27	769.2762599	833.2685	467.99436	519.2347542	3.00E+04	1.55E+03	5.72E+05	8.32E+05	1.06E+06	4.02E+01	2.30E+05
93	88	28	777.3112942	842.3992	463.15696	514.7359746	3.00E+04	2.03E+03	7.28E+05	1.10E+06	1.40E+06	4.00E+01	2.91E+05
93	88	29	785.1438878	851.2999	458.53674	510.4391673	3.00E+04	2.86E+03	1.00E+06	1.58E+06	1.98E+06	3.97E+01	3.97E+05
93	88	30	792.7858662	859.9839	454.11694	506.328755	3.00E+04	4.72E+03	1.61E+06	2.65E+06	3.29E+06	3.93E+01	6.34E+05

Pressure Ratio	93/88	Max Efficiency
5		3.03E+01
6		3.26E+01
7		3.44E+01
8		3.58E+01
9		3.69E+01
10		3.79E+01
11		3.86E+01
12		3.92E+01
13		3.97E+01
14		4.01E+01
15		4.05E+01
16		4.07E+01
17		4.09E+01
18		4.10E+01
19		4.11E+01
20		4.11E+01
21		4.11E+01
22		4.11E+01
23		4.10E+01
24		4.08E+01
25		4.07E+01
26		4.05E+01
27		4.02E+01
28		4.00E+01
29		3.97E+01
30		3.93E+01

41.12638394



Solar Tower	Optimal Compression Ratio	Q_h(kW)	Efficiency (%)	DNI(kWh/m²·N)	DNI(kW/m²·N)	M*2
	20	2.26E+05	4.11E+01	3.14	0.1308333	17279.28 1727928

Appendix C: CCGT Efficiency Calculations

Below is the MATLAB for the full CCGT efficiency calculations.

```
1 clc
2 clear all
3
4
5 %%% Rankine Cycle claculations (temperatures in Celsisus, pressure in bar)
6
7 % known variables
8 P67=10;
9 P98=.07384;
10 x4=.88;
11 T7=400;
12 T9=40;
13 h9=XSteam('hL-T',T9);
14 nt=.9;
15 Qb=30*10^6;
16 S9=.5724;
17 D=25*10^-3;
18 L=10;
19 U=1000;
20 Tci=18.3;
21 Tco=21.1;
22 epsilon=.0015*10^-3;
23 Cpw=4.18*10^3;
24 rho=999;
25 mu=1.12*10^-3;
26
27 %solving for lower bound of turbine inlet temp
28 s4f=XSteam('sL-p',P98);
29 s4g=XSteam('sV-p',P98);
30 s4=(1-x4)*s4f+x4*s4g;
31
32
33 %solving for the boiler
34 T6=XSteam('T-ps',P67,S9);
35 h6=XSteam('h-ps',P67,S9);
36 h7=XSteam('h-pT',P67, T7);
37 m_dot=Qb/(h7-h6);
38
39 % solving the turbine portion of the problem
40 S7=XSteam('s_pT',P67,T7);
41 h8s=XSteam('h-ps',P98,S7);
42 h8=nt*(h7-h8s)+h7;
43 Wt=m_dot*(h8-h7);
44
45 %solving for Rankine pump
46 Wp1=m_dot*(h6-h9);
47
48 %energy balance to find Qc
49 Qc=Qb+Wp1-Wt;
50
51 %solving for condenser
52 Δ_T9=abs(T9-Tci);
```



```

53 Δ_T6=abs (T9-Tco);
54 Δ_T=(Δ_T9-Δ_T6)/(log(Δ_T9/Δ_T6));
55 N=Qc/(U*Δ_T*pi*D*L);
56
57
58 %finding major loss and friction coefficient
59 m_dot_cooling_total=Qc/(Cpw*(Tco-Tci));
60 m_dot_cooling=m_dot_cooling_total/N;
61 V=(m_dot_cooling)/(rho*pi*(D/2)^2);
62 Reynolds= (rho*V*D)/mu;
63 f=((1)/(-1.8*log10(((epsilon/D)/3.7)^1.11*(6.9/Reynolds))))^2;
64 Maj_loss=((f*L*rho*V^2)*N)/(2*D);
65
66 %cooling pump
67 flow_rate=V*pi*(D/2)^2;
68 Wp2=flow_rate*Maj_loss;
69
70 %overall rankine efficiency
71 nth= (Wt-Wp1-Wp2)/Qb;
72
73 %output array building
74
75 %%% Brayton portion of the calculations (Temperatures in Kelvin, pressure in Pa)
76
77 %known variables
78 T1=300;
79 T3=1200;
80 T5=500;
81 P145=100000;
82 ntb=.93;
83 ncb=.88;
84 k=1.4;
85 Cpa=1.004;
86 rp=9;
87 Ah=100;
88 DNI=3.14/24;
89 %solving for T4 and T4s from the turbine to get m dot
90 T4s=T3*(1/rp)^((k-1)/k);
91 T4=ntb*(T4s-T3)+T3;
92 m_dot_brayton= Qb/((Cpa)*(T4-T5));
93
94 %solving for work prouced by the turbine
95 Wtb=m_dot_brayton*(Cpa)*(T3-T4);
96
97 %solving for T2 and T2s to get work used by the compressor
98 T2s=T1*(rp)^((k-1)/k);
99 T2=(T2s-T1)/ncb+T1;
100 Wcb=m_dot_brayton*(Cpa)*(T2-T1);
101
102 %solving for the thermal energy from the heater
103 Qh=m_dot_brayton*(Cpa)*(T3-T2);
104
105 %solving for the number of heliostats required to produce Qh
106 N=(Qh*10^-3)*(1/DNI)*(1/Ah);
107
108 %Total Power output
109 Tot_power=(Wt+Wtb-Wcb-Wp1-Wp2);

```

```
110
111 %Total cycle efficiency
112 cycle_efficiency=Tot_power/Qh
```

Appendix D: Heat Exchanger Calculations

Below is the MATLAB for the heat exchanger heat transfer, length, and critical heat flux calculations.

```
1 clc
2 clear all
3
4 %Known Temperatures/pressures for heat exchangers (temperature in celsius,
5 %pressure in bar)
6 T4=679.6943-273.15;
7 T5=500-273.15;
8 T6=40.0228;
9 T7=400;
10 P67=10;
11 P45=1;
12 m_dot_vapor=9.69;
13 m_dot_air=30E3/(T4-T5);
14
15
16 %%%Calculations for overall Q
17 %superheater
18 Qs=m_dot_vapor*(XSteam("h_pT",P67,T7)-XSteam("hV_p",P67));
19 %preheater
20 Qp=m_dot_vapor*XSteam("CpL_p", P67)*(XSteam("Tsats_p",P67)-T6);
21 %evaporator
22 Qe=m_dot_vapor*(XSteam("hV_p",P67)-XSteam("hL_p",P67));
23 %total
24 Q_tot=Qe+Qp+Qs
25
26 %%%Calculations for lengths
27 %%% superheater
28 %known/easily found stuff
29 pr_air=.690;
30 pr_vapor=1.05; %take average between the two
31 Dh=(80-50)*10^(-3);
32 k_air=26.3e-3;
33 k_vapor=(40.5e-3);
34 Cp_air=1.004; %assuming air is an ideal gas
35 Cp_vapor=(XSteam("CpV_p",P67)+XSteam("Cp_pT",P67,180))/2;
36 density_air=1.169;
37 density_vapor=(XSteam("rho_pT",P67,T7)+XSteam("rhoV_p",P67))/2;
38 N=200;
39 A_air_s=pi*(25e-3)^2;
40 A_vapor_s=(pi*((40e-3)^2-(25e-3)^2));
41 dynamic_air=2.573e-5;
42 dynamic_vapor=(XSteam("my_pT",P67, T7)+XSteam("my_pT", P67, 180))/2;
43
44 T4b=T4-(Qs/(m_dot_air*Cp_air));
45 U_m_air_s=m_dot_air/(density_air*(A_air_s)*N);
46 U_m_vapor_s=m_dot_vapor/(density_vapor*(A_vapor_s)*N);
47 Re_air_s=((density_air*U_m_air_s*50e-3)/dynamic_air);
48 Re_vapor_s=((density_vapor*U_m_vapor_s*(30e-3))/dynamic_vapor);
49 Nu_air_s=(.023)*(Re_air_s)^(4/5)*(pr_air)^(.4);
50 Nu_vapor_s=(.023)*(Re_vapor_s)^(4/5)*(pr_vapor)^(.3);
51 h_vapor_s=(Nu_vapor_s*k_vapor)/(30*10^(-3));
52 h_air_s=(Nu_air_s*k_air)/(50e-3);
```

```

53 U_s=((1/h_air_s)+(1/h_vapor_s))^-1;
54 Delta_T1_s=T4b-XSteam("Tsats_p",P67);
55 Delta_T2_s=T4-T7;
56 Delta_Lm_s=(Delta_T1_s-Delta_T2_s)/log(Delta_T1_s/Delta_T2_s);
57
58 Ls=(Qs*10^3)/(U_s*Delta_Lm_s*N*(pi*(50e-3)));
59
60
61 %%%Evaporator
62 %Pool boiling so only air needs to be accounted for in h for U
63 %same process as superheater
64 A_vapor_e=A_vapor_s;
65 A_air_e=A_air_s;
66 T4c=T4b-(Qe/m_dot_air*Cp_air);
67 U_m_air_e=U_m_air_s;
68 Re_air_e=Re_air_s;
69 Nu_air_e=Nu_air_s;
70 h_air_e=h_air_s;
71 U_e=(1/h_air_e)^-1;
72 Delta_T1_e=T4c-XSteam("Tsats_p",P67);
73 Delta_T2_e=T4b-XSteam("Tsats_p",P67);
74 Delta_Lm_e=(Delta_T1_e-Delta_T2_e)/log(Delta_T1_e/Delta_T2_e);
75
76 Le=(Qe*10^3)/(U_e*Delta_Lm_e*N*(pi*(50e-3)));
77
78 %Still need to check that critical heat flux is below the threshold
79 g=9.81;
80 Cz=.131;
81 hfg=2015.29;
82 sigma_lv=42.9e-3;
83 rho_v=XSteam('rhoV_p',P67);
84 rho_l=XSteam('rhoL_p',P67);
85 crit_heat=(Cz*hfg*rho_v)*(((sigma_lv*g*(rho_l-rho_v))/(rho_v^2))^(1/4));
86
87 %actual heat flux
88 h_flux=Qe/(N*pi*(50e-3)*Le);
89
90 %%%Preheater
91 %Need to use epsilon-NTU
92 %know it is a shell and tube with one shell and 2 passes
93 Cp_water_p=(XSteam('CpL_p',P67)+XSteam('Cp_pT',P67,T6))/2;
94 density_water_p=(XSteam('rho_pT',P67,T6)+XSteam('rhoL_p',P67))/2;
95 dynamic_water_p=(XSteam('my_pT',P67,T6)+XSteam('my_pT',P67,179.5))/2;
96 k_water_p=(.673+(.645))/2;
97 pr_water_p=2.384;
98 %
99
100 Qp_max=Cp_water_p*m_dot_vapor*(T4c-T6);
101 C_r=(Cp_water_p*m_dot_vapor)/(Cp_air*m_dot_air);
102 %Q_p2=m_dot_air*Cp_air*(T4c-T5);
103 epsilon=Qp/Qp_max;
104 E=((2/epsilon)-(1+C_r))/((1+C_r^2)^.5);
105 NTU=(-(1+C_r^2)^(-.5))*log((E-1)/(E+1));
106 Dp=20e-3;
107 SD=1.5*Dp;
108 D_square=(19*SD)+Dp;
109 D_shell=sqrt(D_square^2+D_square^2);

```

```

110 bs=.35*D_shell;
111 Sm=(bs)*(SD-Dp);
112 Gs=(m_dot_air)/(Sm);
113 De=(4*(1*SD^2-((pi*Dp^2)/4)))/(pi*Dp); %assuming square pitch so Cpd=1
114 Res_air_p=(De*Gs)/(dynamic_air);
115 Nu_air_p=.36*(Res_air_p^.55)*(pr_air^(1/3));
116 h_air_p=(k_air*Nu_air_p)/Dp;
117 Re_water_p=(4*m_dot_vapor)/(pi*Dp*dynamic_water_p*N);
118 Nu_water_p=.023*(Re_water_p^(4/5))*(pr_water_p)^(.4);
119 h_water_p=(Nu_water_p*k_water_p)/(Dp);
120 U_p=((1/h_air_p)+(1/h_water_p))^-1;
121
122 Lp=(NTU*Cp_water_p*m_dot_vapor*1000)/(U_p*pi*Dp*N)

```